

Geology, Geochronology and Mineralization of the Chilanko Forks to Southern Clusko River Area, West-Central British Columbia (NTS 093C/01, 08, 09S)

by M.G. Mihalynuk, E.A. Orovan¹, J.P. Larocque², R.M. Friedman³ and T. Bachiu⁴

KEYWORDS: regional geology, structure, litho-geochemistry, mineral potential, Clusko River, Chilanko Forks, Chilcotin River, mountain pine beetle

INTRODUCTION

In 2008, the Beetle Impacted Zone (BIZ) project focused on bedrock mapping and resource evaluation of the Chilanko Forks (NTS 093C/01) and Clusko River (NTS 093C/09S) map areas. Located between Williams Lake and Bella Coola, in the Anahim Lake area, these map areas were targeted because of relatively good logging road access and a historical lack of mineral exploration. Building upon mapping completed in 2007 in the intervening Chezacut map area (NTS 093C/08; Mihalynuk et al., 2008a, b), results of new revision mapping in the Clusko River sheet to the north and Chilanko Forks sheet to the south are presented here, together with results from isotopic age investigation of Chezacut area map units.

Mapping and resource evaluation in 2007 demonstrated that rock exposures are more extensive and Chilcotin basalt is less extensive than previously recognized, and that further mineral exploration in the Anahim Lake region is warranted. Results of the 2008 field program echo these findings, providing further incentive for future mineral exploration in the region.

The BIZ project is one facet of a broad effort by the provincial government to stimulate economic diversification and to help reduce the long-term negative economic impact of the mountain pine beetle. As recorded by the 2004 Forest Health Survey (BC Ministry of Forests and Range, 2005a), the area of contiguous pine beetle infestation at that time was nearly coextensive with the Interior Plateau (Figure 1). Historically unprecedented in size, the beetle infestation will lead to an inevitable degradation of the trees available to the forest industry for harvest and a deceleration of the chief economic engine in central British Columbia (Ministry of Forests and Range, 2005b).

PINE BEETLE BACKGROUND

In western North America, mountain pine beetles range from northern BC to northern Mexico. Across the interior of BC, the forest ecosystem is dominated by lodgepole pine, which at around 80 years of age, reach their maximum susceptibility to mountain pine beetle attack (Shore and Safranyik, 1992). At the outset of the current pine beetle epidemic, more than half of the pine forest stands in BC were near optimal susceptible age, largely as a consequence of fire suppression efforts. Fire suppression by government agencies was an outgrowth of the Dominion Forest Reserves Act of 1906 (Taylor, 1999) and creation of the BC Forest Service Protection Branch in 1912 (BC Ministry of Forests and Range, 2008). Particularly effective fire suppression measures have been invoked since the 1960s, such that by 2004 mature pine forest was three times as abundant as it would be in an unmanaged state (55% versus ~17%; Taylor and Carroll, 2004). Today, the BC Forest Service Protection Branch reports an initial attack fire suppression success rate of 92% (BC Ministry of Forests and Range, 2008).

The current mountain pine beetle epidemic is one of five recorded outbreaks within the past 85 years (Taylor and Carroll, 2004), although evidence for mountain pine beetle infestations extends to centuries past in the form of tree ring scars (Alfaro et al., 2004). Precise distribution and severity of infestations have been recorded only since the beginning of comprehensive aerial surveys in 1959 (e.g., Taylor and Carroll, 2004).

LOCATION AND ACCESS

Geological bedrock mapping completed in 2008 covered an area of ~1300 km², located approximately 200 km west of Williams Lake, midway on the Highway 20 route to Bella Coola. It includes the resort community of Puntzi Lake, a former military air base on the northern side of Highway 20 (Figure 1). Just outside the eastern map border, along Highway 20, is the community of Redstone (20 km west of the official location shown on most maps).

Six main forest service roads provide access to the map areas (Figures 1, 2). Two main roads service the Clusko River area: the Chezacut (100) Road crosses the area diagonally from the southeast (also known as the Clusko River-Thunder Mountain Road beyond the Clusko River), and a major branch known as the Scotty Meadow Road crosses the northeastern map area. Four of the main roads service the Chilanko Forks area: the Baldwin Lakes Road and the 5600 Road extend into the south-central and southeastern portion of the map area, the Clusko Main accesses the southwest, and the Puntzi Lake Road transects the south-

¹ Carleton University, Ottawa, ON

² University of Victoria, Victoria, BC

³ Pacific Centre for Isotopic and Geochemical Research, University of British Columbia, Vancouver, BC

⁴ Dalhousie University, Halifax, NS

This publication is also available, free of charge, as colour digital files in Adobe Acrobat® PDF format from the BC Ministry of Energy, Mines and Petroleum Resources website at <http://www.empr.gov.bc.ca/Mining/Geoscience/PublicationsCatalogue/Fieldwork/Pages/default.aspx>.

central and western parts of the map area. In the Clusko River area, low elevation roadbeds are partly constructed on glaciolacustrine deposits, which can become greasy and treacherous when rain-soaked. Hundreds of kilometres of secondary logging roads branch off the major forestry service roads, although many of these are deactivated and best accessed by mountain bike or on foot. On old logging roads or in open pine forest with sparse outcrop, foot traverses in excess of 20 km are routine.

REGIONAL GEOLOGICAL SETTING AND PREVIOUS WORK

The Clusko River and Chilanko Forks areas are part of the Fraser Plateau (Figure 1; south-central Interior Plateau as defined by Holland, 1964). Basement rocks in this area are part of southeastern Stikine terrane, a Devonian to Jurassic arc complex, near its eastern contact with the Cache Creek terrane, a Mississippian to Early Jurassic accretionary complex. Subsequent to Middle Jurassic amalgamation of these two terranes (e.g., Ricketts et al., 1992; Mihalyuk et al., 2004), the contact was overlapped by Late Jurassic volcano-sedimentary strata, perhaps correlative with the late Jurassic Nechako/Fawnie volcanic rocks of Diakow et al. (1997) and Diakow and Levson (1997).

The southern Clusko River map area is underlain almost exclusively by supracrustal Eocene continental arc volcanic strata deposited during ~55–47 Ma extensional exhumation and cooling of kyanite-grade basement rocks characterized by ~107 Ma deformational fabrics (Friedman, 1992). Upper crustal equivalents of these Mesozoic basement rocks are well-exposed in the Chezacut and Chilanko Forks areas. Miocene, Neogene and Quaternary volcanic rocks drape the post-Eocene paleotopography and volcanic flows infill paleotopographic lows. Larocque and Mihalyuk (2009) have examined the petrogenesis of the Miocene and younger rocks in greater detail.

Previous regional bedrock geological mapping in the Anahim Lake area was conducted by Tipper (1969a; 1:250 000 scale, NTS 093C). In the Clusko River area, Tipper's mapping was revised by Metcalfe et al. (1997; 1:50 000 scale, published at approximately 1:350 000 scale, NTS 093C/09, 16, 093B/12, 13), who focused on volcanology and epithermal mineralization in the Eocene volcanic rocks. To the immediate west and south, the Tatla Lake Metamorphic Complex was mapped by Friedman (1988; 1:50 000 and 1:20 000 scales) as part of a Ph.D. study on its structural exhumation. His mapping was extended farther southwest by Mustard and van der Heyden (1997; 1:50 000 scale, NTS 092N/14E, 15). All of these sources of bedrock map data have been compiled by Massey et al. (2005) as part of the digital provincial geology map, and by Riddell (2006) to aid with petroleum resource assessment. Modern geophysical studies include the reprocessing of seismic data from hydrocarbon exploration activity undertaken in the Interior Plateau in the early 1980s (e.g., Hayward and Calvert, 2008), as well as the acquisition and interpretation of new geophysical surveys, including passive seismic tomography (e.g., Cassidy and Al-Khoubbi, 2007) and magnetotelluric imaging (e.g., Spratt and Craven, 2008).

Two main periods of hydrocarbon exploration activity, in the early 1960s and 1980s, resulted in more than 12 exploration wells drilled in the volcano-sedimentary strata,

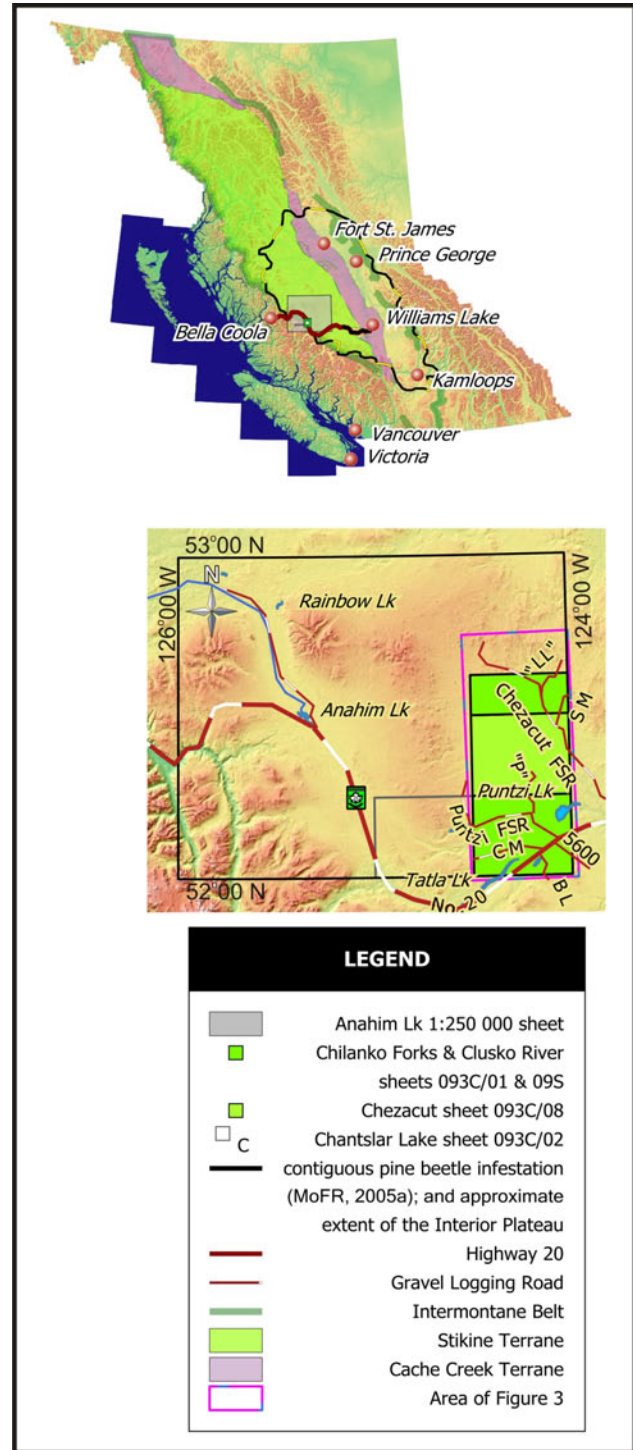


Figure 1. Location of the Chilanko Forks and Clusko River map area, showing features mentioned in the text. Also shown are: the area of 2005 mountain pine beetle infestation, which is nearly co-extensive with the Interior Plateau (the southern half of which is the Fraser Plateau; Holland, 1964), distribution of Stikine and Cache Creek terranes (Massey et al., 2005), and the extent of the Intermontane Belt. Road abbreviations: BL, Baldwin Lakes; CM, Clusko Main; FSR, Forest Service Road; SM, Scotty Meadow, see text.

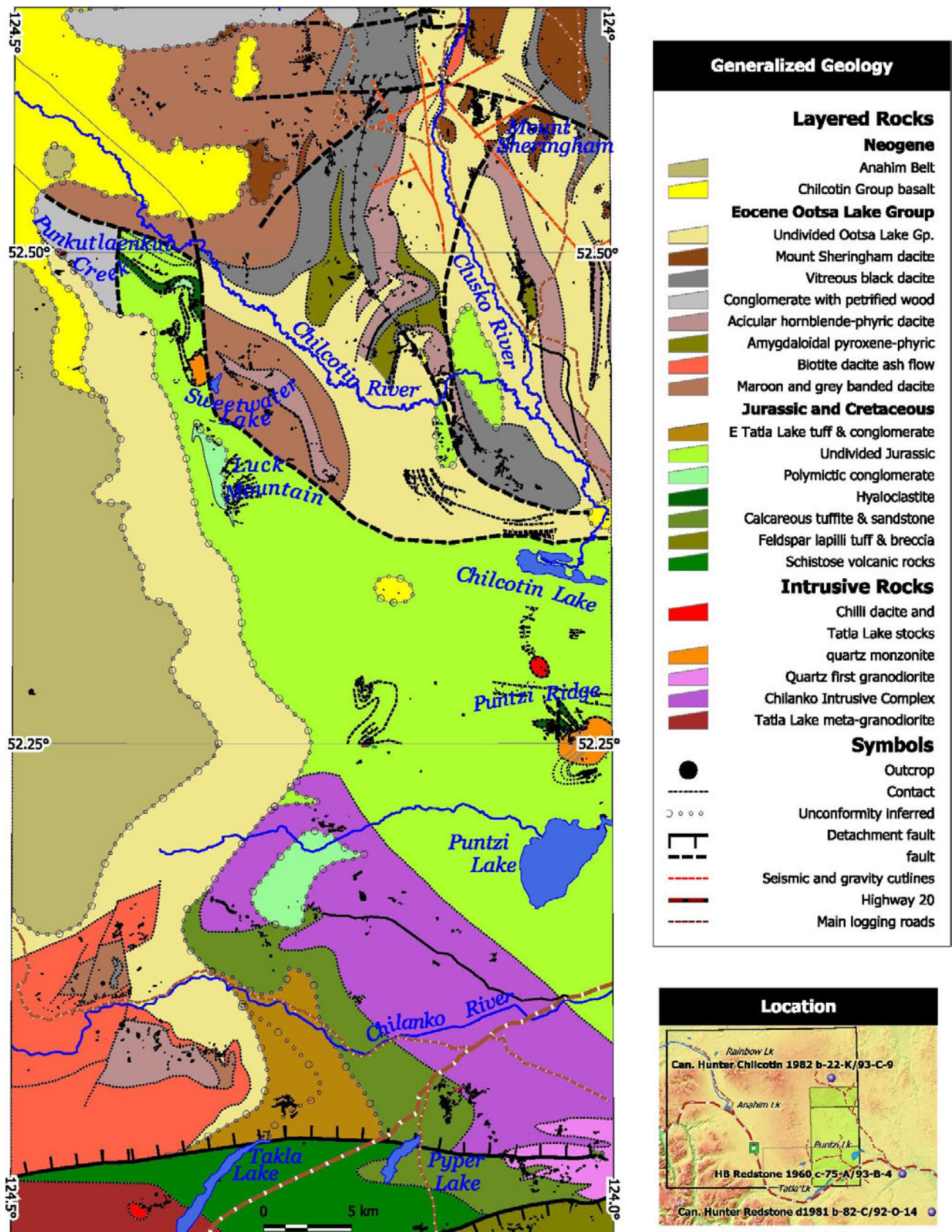


Figure 2. Geological sketch map showing the distribution of major units discussed in the text, new and existing showings, major access roads and sampling sites. This figure incorporates geological map data from Tipper (1969a), Massey et al. (2005), Riddell (2006) and Mihalynuk et al. (2008a).

which overlap the Stikine–Cache Creek terrane boundary (see Ferri and Riddell, 2006 for a chronology of hydrocarbon exploration). Seven of those wells have cores available for inspection at the BC Ministry of Energy, Mines and Petroleum Resources Core Facility located at Charlie Lake (Mustard and MacEachern, 2007). Three of these, from wells located 7 km north, 30 km east and 54 km southeast of the map area (see Figure 2), provide data down to 3778 m (Canadian Hunter Chilcotin 1982, b-22-K/93-C-9), 1307.5 m (Hudson Bay Redstone 1960, c-75-A/93-B-4), and 1720 m (Canadian Hunter et al. Redstone 1981, b-82-C/92-O-14). Riddell et al. (2007) reported palynological and age data from samples of the latter two wells: Late Albian palynomorphs from marine shale from 115 to 152 m underlain by marine to terrestrial strata of probable Middle to Late Albian age and, in the other well, Late Albian or Cenomanian palynomorphs from between 1210 and 1610 m. In an excellent synopsis of age and stratigraphic data, Riddell et al. (2007) report isotopic age data from the granitoid at the maximum depth penetrated (1730 m) by Canadian Hunter et al. Redstone b-82-C as 101.4 ± 1.9 Ma, and a detrital age from clastic strata at 635–730 m of 101.7 ± 2.2 Ma.

An Early to Middle Eocene U-Pb zircon age was obtained from volcanic rocks cored at 3121 m in Canadian Hunter Chilcotin b-22-K, essentially the same as three detrital zircon ages obtained from samples collected at depths of between 2000 and 3745 m. If the strata penetrated by Chilcotin b-22-K have not been structurally thickened, the data reported in Riddell et al. (2007) indicate an Eocene volcano-stratigraphic thickness in excess of 3745 m.

Regional glacial and fluvial physiography and surficial deposits have been mapped across the Anahim Lake area by Tipper (1971) and in more detail in the eastern Anahim Lake area by Kerr and Giles (1993; NTS 093C/01, 08, 09, 16), who also conducted till geochemical surveys (see Levson and Giles, 1997). Similarly detailed surficial surveys were conducted by Ferbey et al. (2009) in the area immediately to the east (NTS 093B/03, 04). Mihalyuk et al. (2008b) postulated that a late glacial lake occupied most valleys in the Chezacut area at elevations below 1154 m.

FIELD TECHNIQUES

Field mapping in 2008 adapted techniques that were found to be beneficial in 2007. In particular, 1:20 000-scale digital orthophotographs (0.5 m resolution) were used extensively for the identification of areas of outcrop and definition of geological lineaments. Roadcuts added to the inventory of bedrock exposures, but only marginally. For example, rocks exposed within 15 m of roads constitute only 1.4% of those mapped within the Clusko River area, or even less than the meagre 2.4% in the Chezacut area (Mihalyuk et al., 2008b; Figure 2). Thus, mapping focused along road networks creates a falsely negative impression of the percentage of outcrop within the area. It is no accident that roads are preferentially constructed so as to avoid the high costs of blasting bedrock. Across the region, the most extensive outcrop exposures are along glacially scoured ridges and along the margins of glacial meltwater channels that are visible on 1:20 000-scale orthophotographs.

In areas with extensive till cover, clast compositions can be used as a guide to the underlying geology. Unfortunately, this technique is reliable only for basal till, whereas

the most extensive surficial cover deposits in the area mapped in 2008 are reworked glaciofluvial or potentially far-travelled hummocky glacial deposits. Contacts between units with a high magnetic contrast can be reliably mapped in the subsurface using available aeromagnetic survey data (Figure 3), as was done to create Figure 2.

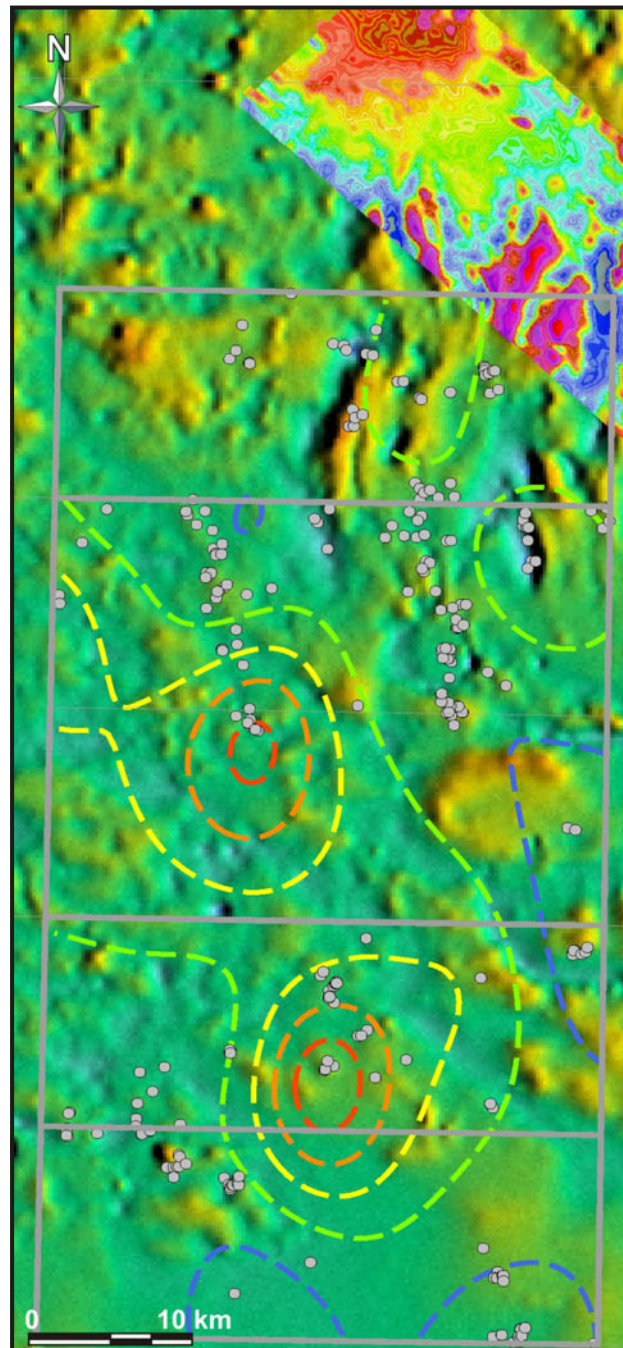


Figure 3. Regional aeromagnetic survey shaded total field (Geological Survey of Canada, 1994) and higher resolution total field coverage in northeastern portion of NTS 093C/09S from the Clisbako multiparameter survey; see Figure 1 for location. Overlain contoured magnetic susceptibility values range from 5 to 25, with an interval of 5 SI units. Locations of magnetic susceptibility measurements at the outcrop are shown as grey dots.

LAYERED ROCKS

Layered rocks within the Chezacut map area were divided into four successions: Mesozoic, Eocene, Oligocene-Pleistocene or Pleistocene-Holocene by Mihalynuk et al. (2008b). Many of the units that constitute these successions extend into the current map areas (Figures 2, 3); they were described by Mihalynuk et al. (2008b) and are, therefore, not repeated here. However, units that significantly change character or may bear upon a different interpretation are described below.

Mesozoic

Poorly fossiliferous Mesozoic strata were presumed by Tipper (1969a) and Mihalynuk et al. (2008b) to correlate with Late Triassic and Early Jurassic Stikine terrane volcanic arc strata. However, some strata in the Chilanko Forks area are now known to be Middle Jurassic or perhaps as young as mid-Cretaceous in age, and belong to overlap successions that are of particular interest for their hydrocarbon resource potential (e.g., Riddell and Ferri, 2008). For example, the only known fossil age determination in the Chilanko Forks area is from tuffaceous mudstone on the northern shore of Puntzi Lake (GSC locality 79765). Following publication of the Anahim Lake map in 1968, Tipper (1969b) reported that it contained poorly preserved Middle Jurassic ammonites: “According to H. Freebold a probable Bajocian age is indicated” (Tipper, 1969b, page 23). The ammonite-bearing tuffaceous mudstone unit is part of a coherent stratigraphy intruded by monzonite, for which we report a new Middle Jurassic isotopic age determination (see ‘Geochronology’ below). Coherent Mesozoic strata are common within the Chezacut area, extending from Puntzi Ridge to Puntzi Lake, in the northeastern corner of the Chilanko Forks sheet, but are not exposed farther south and east. Similar strata are expected to extend into the ~6 km² of the far southwestern corner of the southern Klusko River map area (Punkutlaenkut Creek-Chilcotin River confluence), but field conditions did not permit access to this area, which falls outside the limit of mapping shown in Figure 2. Partly correlative strata cut by, and deformed together with, a variably foliated polyphase tonalite to basaltic intrusive complex underlie much of the remaining portion of the Chilanko Forks area, except for the southeastern corner, which is underlain by Mesozoic (?) massive volcanic breccia. Another exception, the west-central part of the map area, is underlain by Eocene dacitic strata of the Ootsa Lake Group.

Map units characteristic of the coherent Mesozoic strata include: a bright green, carbonate-cemented, hyaloclastic lapilli tuff; indurated, tan and brown volcanic siltstone; orange, ‘monzonitic’ crystal lapilli tuff; and pyritic, coarse rhyolite breccia. All of these units are described in Mihalynuk et al. (2008b); units not previously described follow.

BAJOCIAN TUFFACEOUS SILTSTONE

Low, recessive, friable outcrops of red-brown tuffaceous mudstone to sandstone (Figure 4a) crop out low



Figure 4. Mesozoic rock types, including a) well-bedded outcrop of Bajocian tuffaceous siltstone, b) massive volcanic breccia displaying typical rectilinear epidote-quartz-chlorite vein sets, and c) granule conglomerate portion of calcareous tuffite and sandstone.

on the southern flank of Mount Palmer and northern shore of Puntzi Lake. Mudstone appears to be interbedded with finely feldspar-phyric flows <2 m thick. Outcrops are strongly fractured and calcite veined, such that contact relationships are uncertain. Some 'flows' could in fact be dikes or unusually uniform, water-lain tuff that lacks significant winnowing or sorting.

VARIEGATED SILICEOUS TUFF AND RHYOLITIC FLOWS

Rusty, white-weathering outcrops form resistant ridges, and range from coarse breccia to possible flow domes. The flows and pyroclastic rocks are typically well-indurated, with silicified clasts showing ochre, white and/or dark green ghosted margins. Thickness varies, but exposures are typically in the order of tens of metres thick. Pyritic zones are common, and pyrite can exceed 5% by volume of the rock over widths of a metre.

VEINED MASSIVE TUFF

Bright green, extensively epidote-altered, blocky, orange-weathering and resistant breccia and lapilli tuff crop out across ~20 km² of southeastern NTS 093C/01. A presumably more distal lapilli- and ash tuff-dominated facies crops out sporadically north of Fit Mountain. Minor chlorite amygdaloidal flows and epiclastic strata are locally important. A feldspar crystal ash matrix is common in all tuffaceous facies. Medium-grained feldspar constitutes 10–25% of the ash and up to 35% of most fragments. Up to 5% of the rock may consist of chloritized hornblende, occurring as medium-grained subidiomorphic crystals. Sparse, altered pyroxene may also be present, but it has not been confirmed petrographically.

Green volcanic strata are locally interlayered with maroon, typically more ash-rich and breccia-poor layers <~20 m thick. In some of these layers, vague clast sorting and rounding suggest an epiclastic origin, but most contain highly angular fragments. Strain is commonly partitioned into these finer-grained units.

Extensive epidote-chlorite and quartz veining is characteristic of the massive blocky parts of the unit. Epidote-quartz veins commonly form parallel sets of veins which may range from 1 mm to ~4 cm in thickness, and are well developed across vein strike for 10 m or more (Figure 4b).

CALCAREOUS TUFFITE AND SANDSTONE

Perhaps the most widespread Mesozoic sedimentary unit exposed in the Chilanko Forks-Clusko River map area is grey to blue-green volcanic tuffite and sandstone, commonly with a calcareous matrix. This unit is texturally variable, ranging from green sandstone with granule-conglomerate lags (Figure 4c) to epiclastic units with tuffaceous interbeds, to dark grey phyllitic mudstone. Limestone layers up to 10 cm thick have been observed in two localities. If better exposed, this unit could probably be subdivided into several mappable units.

The best exposures of this unit are on the hills east of Pyper Lake and in the thermal metamorphic halo of the Clusko Intrusive Complex near Puntzi Mountain. Adjacent to the complex, the carbonate matrix has been consumed through the production of secondary calcsilicate minerals: epidote or actinolite/tremolite, and rare grossular garnet.

Correlative units within the Chezacut map area (near Arc Mountain) may be the 'calcareous fossiliferous sand-

stone', 'volcanic siltstone/sandstone' and possibly, the 'calcareous chert pebble conglomerate' described in previous work (Mihalynuk et al., 2008b). Such variability in correlative units might be expected given that they are separated from those in the Chilanko Forks map area by more than 25 km.

A minimum relative age constraint on this unit is provided by the crosscutting, pre- to syndeformational Clusko Intrusive Complex. Two samples of this complex have been submitted for isotopic age determination, but neither has been completed as this paper goes to press. However, a new U-Pb age determination from the mainly undeformed 'Puntzi Ridge quartz monzonite', which cuts the presumably correlative strata within the Chezacut map area, is reported below as 160.94 ± 0.13 Ma.

Cretaceous Volcanic Rocks

Volcanic rocks of Cretaceous age have not been directly dated within the Chilanko Forks to southern Clusko River area. However, Cretaceous volcanic strata are dated at 101 ± 2 Ma immediately east of the map area at Puntzi Lake, as reported by Riddell and Ferri (2008). Regionally, these rocks may correlate with the Spences Bridge Group (Thorkelson and Rouse, 1989; Diakow and Barrios, 2009). Undated volcanic rocks north of eastern Tatla Lake possibly belong to this package, as may rocks that underlie Mount Charlieboy on the southern boundary of the Chezacut map area.

EAST TATLA LAKE TUFF AND AUTOBRECCIA

Olive-green or maroon, blocky to rubbly and orange- to tan-weathering tuff and breccia crop out north of the eastern end of Tatla Lake. They are vesicular and contain 20% by volume of medium- to coarse-grained, tabular plagioclase, which is commonly idiomorphic and slightly turbid, but in some outcrops can be vitreous. Vesicles are generally irregularly shaped, chlorite- or quartz-filled, with minor bright green celadonite (Figure 5a). They are less than 5 mm in diameter, and make up 5% by volume (locally up to 25%) of outcrops. Mafic minerals include chloritized biotite, less commonly hornblende, and possibly pyroxene; the latter is typically fine- to medium-grained, idiomorphic and accounts for less than 5%. Most outcrops are cut by calcite and/or zeolite (laumontite [?]) veins.

EAST TATLA LAKE CONGLOMERATE

Very coarse boulder to cobble conglomerate (Figure 5b) with sparse, planar, arkosic volcanic sandstone layers appears to be entirely of local derivation, sourced from the underlying East Tatla Lake tuff and autobreccia. Unusually well-rounded boulders of chloritic, amygdaloidal, coarse-bladed feldspar porphyry flow exceeding 2 m in diameter indicate a persistent, very high-energy fluvial environment of deposition.

Eocene Ootsa Lake Group

Volcanic units that compose the Eocene Ootsa Lake Group in the Chezacut map area were described by Mihalynuk et al. (2008b). These units include: basal conglomerate, acicular hornblende dacite, amygdaloidal pyroxene-phyric basalt, ochre breccia and flow lobes, dacite ash-flow tuff, maroon- and grey-banded rhyolite,

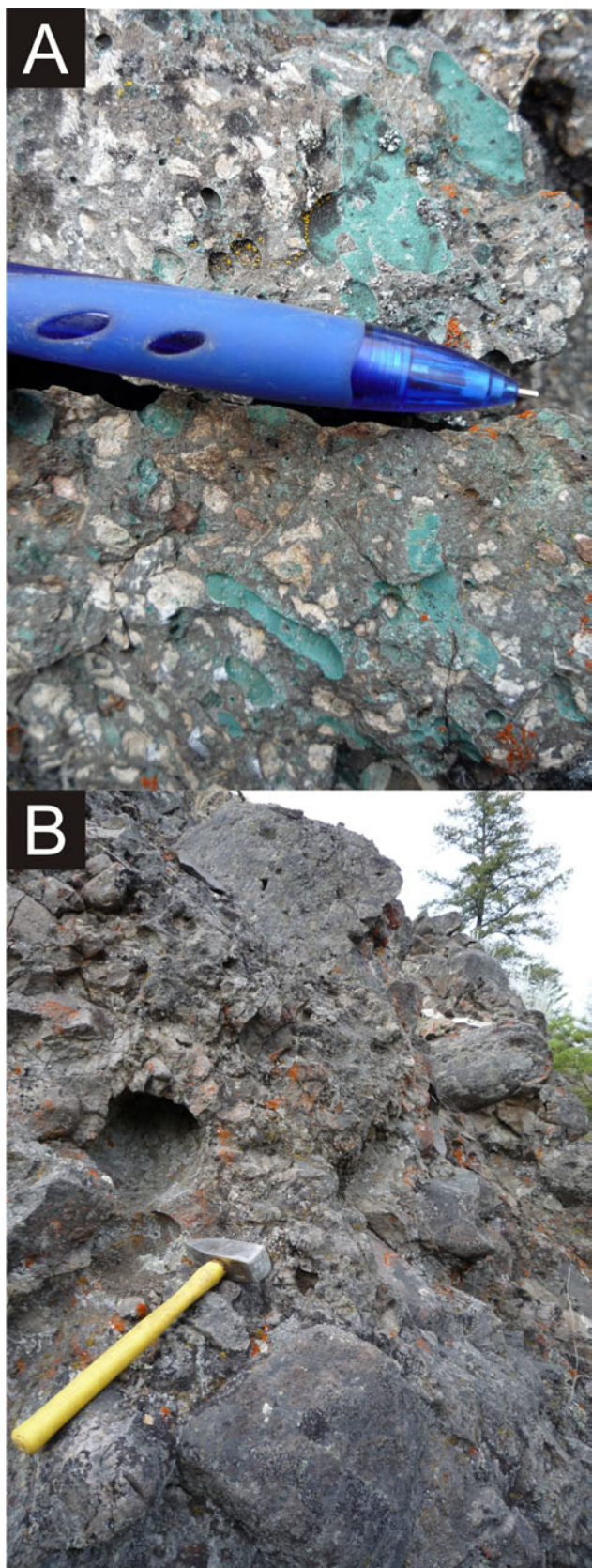


Figure 5. Good exposures of East Tatla Lake a) autobreccia and b) conglomerate.

and vitreous black dacite (Figure 6). Compositions are overwhelmingly dacitic as shown in Figure 7.

Fieldwork in 2008 added two additional units: a conglomerate unit with petrified wood fragments that may occur at several stratigraphic levels, and a variant of the 'vitreous black dacite' unit, that we have named the 'Mount Sheringham pyroxene dacite'.

Seven new $^{40}\text{Ar}/^{39}\text{Ar}$ cooling age determinations for the Ootsa Lake Group within the Chezacut area show that the 'vitreous black dacite' unit is ~46–44 Ma, significantly younger than underlying units (~54–50 Ma); these data are consistent with the geochronological findings of Metcalfe et al. (1997). A full report on age determinations from Ootsa Lake Group volcanic rocks will follow when geochronological data from samples collected in 2008 become available.

POLYMICTIC CONGLOMERATE

Although described by Mihalynuk et al. (2008b), this unit is included here as new observations bear upon the geological interpretation of the area. Bright maroon-weathering, recessive polymictic conglomerate is exposed south and west of Fit Mountain, where it displays an unconformable contact with the late Jurassic Chilanko intrusive complex diorite. Clasts appear to be derived from the underlying Jurassic terrain, including the Chilanko intrusive complex (*see below*). Characteristic maroon soil has developed above and adjacent to the unit. On the basis of local soil colour anomalies, the conglomerate is presumed to underlie an extensive area west and south of Fit Mountain, where it is sporadically exposed. This unit may represent the base of the Eocene succession in the Chilanko Forks area; however, it could also mark the basal contact of the Cretaceous section.

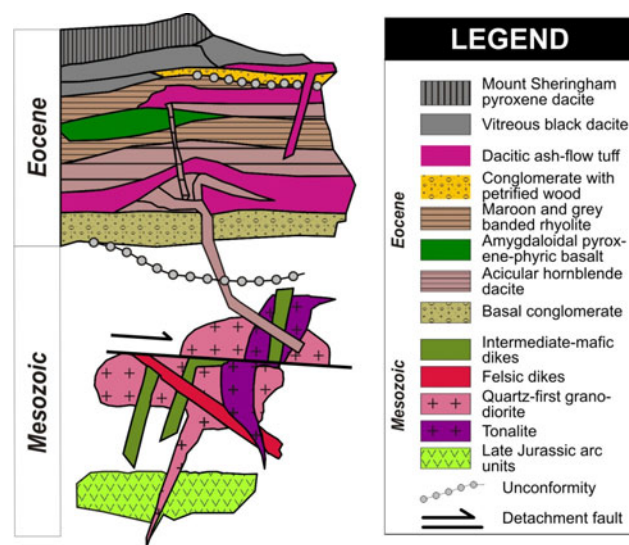


Figure 6. Schematic diagram of stratigraphic relationships between the major units within the Clusko River and Chilanko Forks area. See Mihalynuk et al. (2008b) for stratigraphy of the intervening Chezacut area.

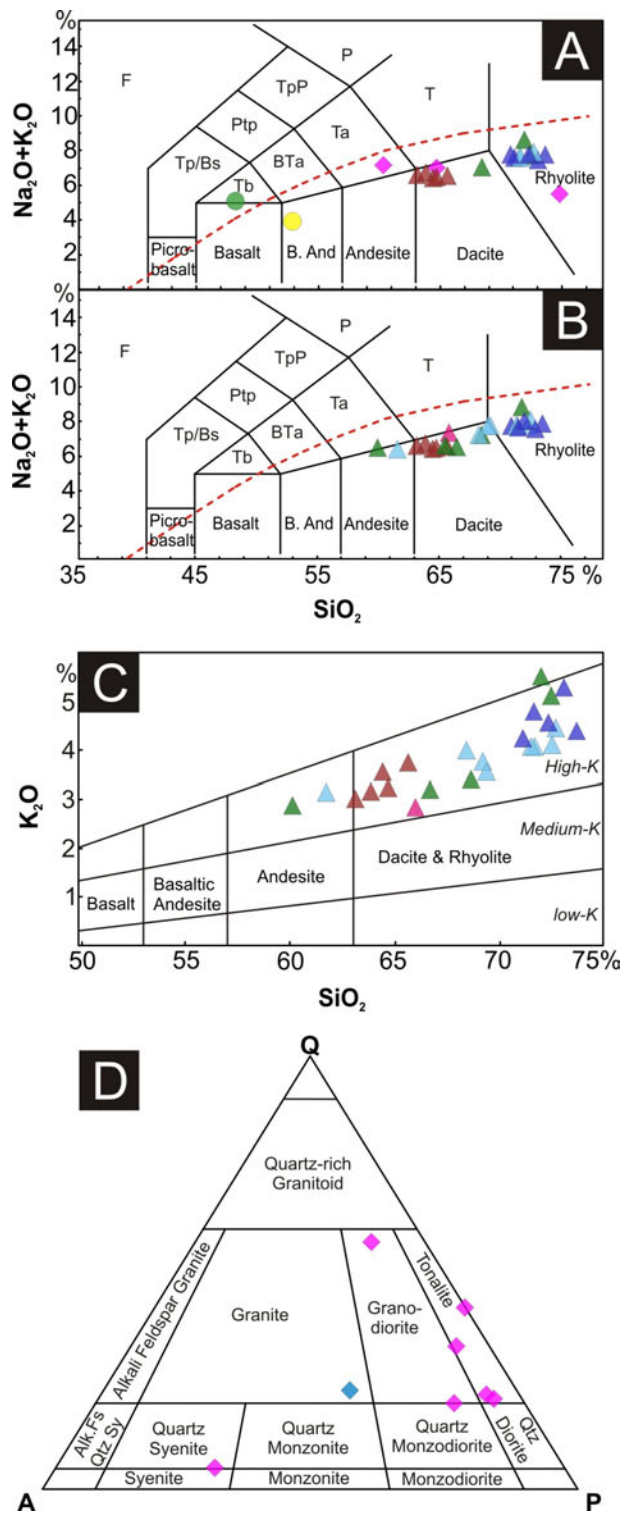


Figure 7. a) Total alkali-silica plot (after Le Maître, 1989) showing all 2008 whole rock samples. **b)** Total alkali-silica plot (after Le Maître, 1989) showing Eocene volcanic rocks from 2007 and 2008. **c)** SiO_2 - K_2O plot for Eocene volcanic rocks from 2007 and 2008. **d)** Quartz-Alkali feldspar-Plagioclase feldspar ternary diagram showing compositions of intrusions mapped in 2008. Compositions are based on visual estimates of phase proportions. F: foidite; P: phonolite; TpP: tephriphonolite; Ptp: phonotephrite; Tp/Bs: tephrite/basanite; T: trachyte; Ta: trachyandesite; Bta: basaltic trachyandesite; Tb: trachybasalt; B.And: basaltic andesite; Alk.Fs Qtz Sy: alkali feldspar quartz syenite.

CONGLOMERATE WITH PETRIFIED WOOD CLASTS

Recessive, rusty, white- to yellow-weathering sandstone and conglomerate are common within the upper part of the Eocene succession near upper Clusko River (Figure 8a). The presence of petrified wood fragments is characteristic of this unit (Figure 8b). In some localities the unit contains bands of indurated, cherty siltstone; in other localities, the conglomerate may be strongly clay-altered and can be carved away by hand. Conglomerate clasts vary in compo-

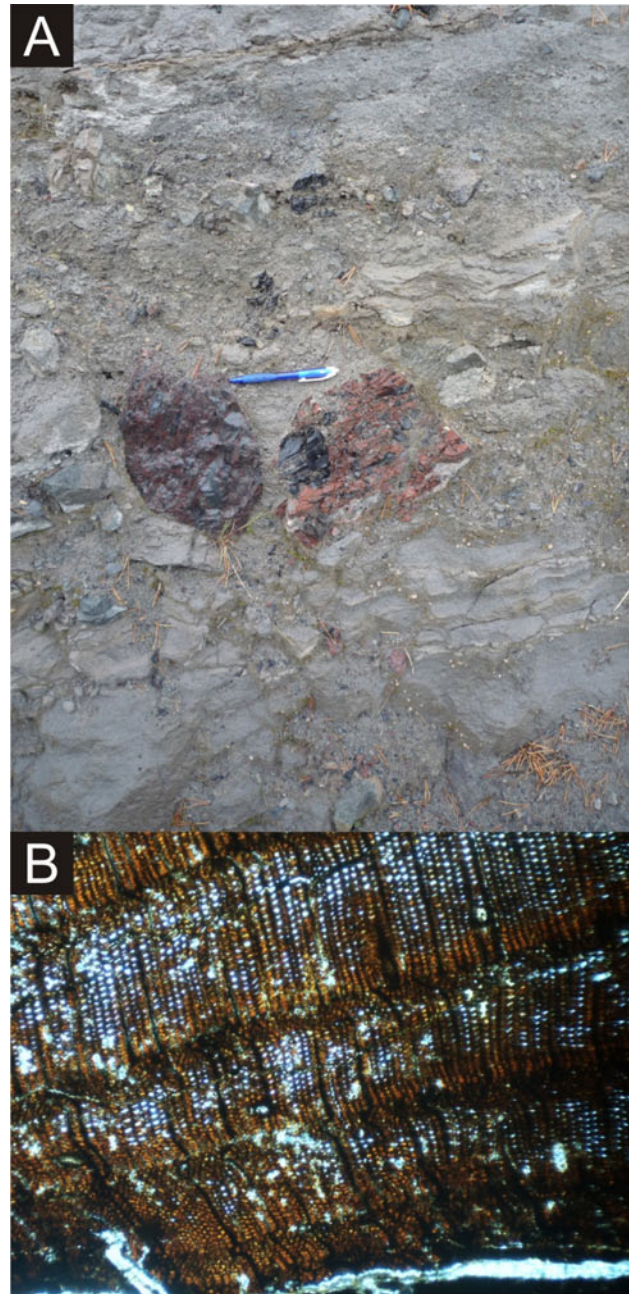


Figure 8. a) Very light grey- to white-weathering epiclastic conglomerate contains vitric ash flow fragments at this locality. **b)** Where the unit is more typically rusty and yellow-weathering, it invariably contains fragments of petrified wood, as seen in the thin section shown here. Long dimension of this photo represents ~2.5 mm.

sition, but quartz-phyric clasts are ubiquitous. Undulating planar bedding and low-angle cross-stratification, and channel lags are common.

MOUNT SHERINGHAM PYROXENE DACITE

Mount Sheringham pyroxene dacite is a subunit of the ‘vitreous black dacite’ of Mihalynuk et al. (2008b) and part of the ‘Pyroxene-bearing Assemblage’ of Metcalfe et al. (1997). However, this unit contains conspicuous, amber to light lime-green quartz eyes, not described as part of the ‘vitreous black dacite’. Colour is imparted to these quartz eyes by a glass-inclusion-riddled rim (Figure 9a), interpreted as being due to a period of rapid crystal growth immediately preceding eruption. Another characteristic of this unit is the formation of spectacular columnar flows that typically range from 1 to 10 m in thickness (Figure 9b) and indicate atypically low viscosity for such a silicic composition (Figure 7).

One previously unreported feature of some amygdaloidal flows that make up the ‘vitreous black dacite’ unit, is the occurrence of a vesicle-filling, fibrous, leather-like mineral (Figure 10). It is preliminarily identified as sepiolite, but this has yet to be confirmed by x-ray diffraction analysis.

Perlitic textures are locally common within the ‘vitreous black dacite’, but none of the perlitic samples tested expanded significantly when heated.

Neogene Volcanic Rocks

Neogene volcanic rocks in the map area encompass two broad rock packages: the Late Oligocene to Early Pleistocene Chilcotin Group, which extends over 35 000 km² of the Interior Plateau (Bevier, 1983; Andrews and Russell, 2007), and the Pleistocene to Holocene Anahim volcanic belt (Bevier, 1989; Mathews, 1989). Their characteristics have been described within the neighbouring Chezacut area (Mihalynuk et al., 2008b) and their geochemistry is the subject of a paper by Larocque and Mihalynuk (2009). Only brief descriptions of one locality within the Chilanko Forks and two within the Clusko River map area follow. Exposures are limited to the far western margin of those areas, although, significant thicknesses of Chilcotin Group basalt crop out immediately east of central Chilanko Forks map area, on the outskirts of Redstone village. Despite the relatively steep Chilanko River valley sides west of Redstone, only glaciofluvial deposits are incised and no bedrock could be found.

DENSE FLOWS

Southwestern-most NTS 093C/09S is underlain by sporadically exposed Chilcotin Group flows. They are typical of the Chilcotin Group: grey with fine- to medium-grained, bright green olivine phenocrysts making up to 3% of the rock. Matrix consists mainly of plagioclase microlites and, locally, 1–2% idiomorphic plagioclase phenocrysts up to 1 cm long. It is characteristically spongy, with intersertal vesicles and glass in approximately equal proportions, together constituting 30% of the rock.

SCORIA DEPOSITS

Just north of the northwestern corner of NTS 093C/09W south half is a steep-sided hill with an apron of unconsolidated black and ochre scoria and ropey bombs (Figure 11) containing fine-grained, zoned plagioclase

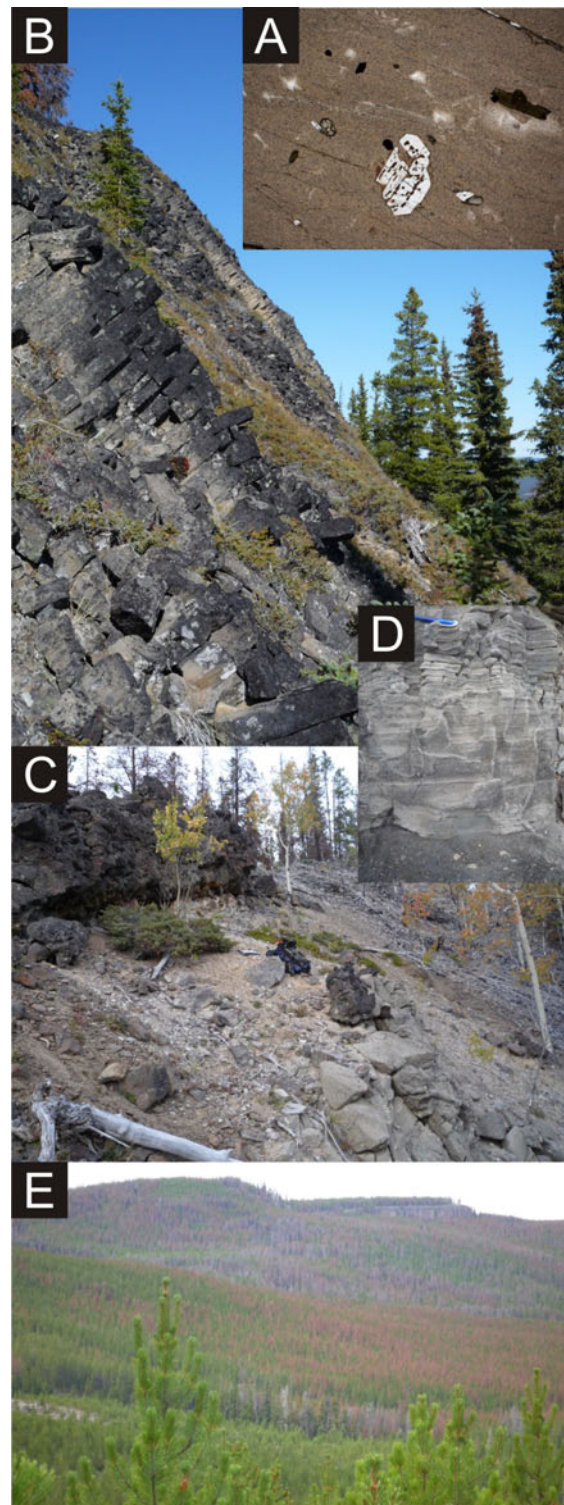


Figure 9. a) Embayed quartz phenocrysts within the Mount Sheringham pyroxene dacite unit display an outer growth zone with abundant glass inclusions. b) An example of well-developed columnar flows typical of this unit. c) Mount Sheringham pyroxene dacite unit sits atop light pink flow-banded dacite (view to the northeast), which pinches out to the south, above light grey epiclastic strata. d) Close-up of epiclastic strata showing trough cross-stratification and planar bedding. e) This unit is 5–10 Ma younger than most of the Ootsa Lake Group and tends to be more flat-lying than older units, as shown by the mesa in the distance.

(15%). Rare blocks contain feldspar phenocrysts up to 2 cm long. Individual blocks are hackly and vesicle-rich (~20%, up to 5 cm) and display little sign of rounding or transport (except for sparse rounded blocks of other rock types on the surface of the scoria apron).

Very low, recessive outcrops on the adjacent hill are composed of jet black scoria and crusty bombs in a poorly lithified, light brown matrix. This bedrock could be the source of scoria, although none of the unconsolidated scoria contain light brown ash matrix within vesicles or adhering to their surfaces. Thus, the scoria apron is interpreted as an essentially primary deposit, perhaps modified slightly by Late Pleistocene meltwater. These deposits are probably part of the young Anahim volcanic belt.

BLOCKY FLOW TOP

Only the low, drift-covered northwestern corner of the Chilanko Forks map area is interpreted as underlain by Neogene volcanic rocks consisting of extensive monolithic block fields interpreted as nearcrop. The blocks are tabular, up to 3 m in diameter and 2 m thick; many of these blocks appear to fit together in jigsaw fashion and are there-



Figure 10. Photomicrograph of fibrous sepiolite (?). Grey, leathery tongues of this mineral developed as it infilled flattened vesicles within flow tops of the 'vitreous black dacite' unit. Long dimension of the photo represents ~2.5 mm.



Figure 11. Scoria deposit in the western half of the Clusko River area (south half).

fore interpreted as part of the same, originally intact, auto-brecciated flow unit. No sign of overlying glacial debris is apparent. Thus, the blocks are interpreted as part of a late to post-Pleistocene unit, perhaps part of the Anahim volcanic belt.

GLACIOGENIC DEPOSITS

Glaciogenic deposits are widespread within the Chilanko Forks area, and are volumetrically dominated by thick glaciofluvial blankets within the main Tatla Lake, Puntzi Creek and Puntzi Lake valleys. Glacial deposits have been discussed as part of a study by Levson and Giles (1997), were mapped by Kerr and Giles (1993), and extend to the east where they were the subject of surficial mapping and till surveys conducted by Ferbey et al. (2009). Readers are referred to these publications for more details.

Glaciolacustrine deposits are preserved sporadically throughout the southeastern Anahim map area. Well-bedded lacustrine strata are exposed along the Clusko River and Puntzi Lake valleys, where they locally exceed 10 m in thickness. In the Chezacut area, they are interpreted as having been deposited by a late glacial lake that inundated approximately 65% of the map area up to an elevation of ~1150 m.

INTRUSIVE ROCKS

Proportional distribution of plutonic intrusive rocks increases southward in the map area, from near zero in the southern half of the Clusko River area to at least 30% in the Chilanko Forks map area. Dikes related to Eocene volcanism are widely dispersed throughout the region, but to the south are greatly outnumbered by those of suspected Jurassic age. In the southeastern map area, swarms of dikes cut a >30 km northwest-elongate polyphase plutonic body that is bisected by the Chilanko River. Collectively, the dikes and pluton are informally referred to as the 'Chilanko intrusive complex'. In the areas mapped, the northwestern limit of the complex is the 'Sweetwater Lake' monzonite, a separate body located in the Chezacut map area.

Chilanko intrusive complex

Tonalite is the most common rock type within the Chilanko intrusive complex (Figure 7), but constituent phases include diorite to granodiorite, monzodiorite and, rarely, granite. Dikes are common, in some places constituting >50% of broad exposures. Dikes range in composition from basalt to felsite and pegmatite of probable granitic composition. Dikes of intermediate composition tend to be the most strongly foliated. Constituent plutonic phases are also commonly foliated. Mafic phases within both plutons and dikes consist of amphibole and biotite, which typically account for less than 10% by volume of the rock, although they may account for as much as 25% (Figure 12a). Subhedral hornblende is often altered to actinolite±chlorite and biotite is commonly pervasively altered to chlorite. Plagioclase varies in habit from tabular euhedral to subhedral and is partly to mostly replaced by white mica, epidote and calcite. It has a composition of $An_{30\pm5}$, although plagioclase as calcic as An_{50} was observed within samples of quartz syenite. Interstitial potassium feldspar is commonly turbid due to very fine-grained clay alteration (probably kaolinite). Quartz typically displays

sutured margins; very quartz-rich samples contain cataclastically reduced quartz grains. Vein assemblages of quartz, calcite, actinolite, epidote and/or prehnite are widespread. Apatite, titanite and zircon are common accessory minerals.

Two plutonic phases within the Chilanko intrusive complex are noteworthy: a uniform body of tonalite at Fit Mountain, and variably foliated quartz-porphyritic granodiorite, herein referred to as the 'quartz-first granodiorite'. Samples of both units were collected for geochronological age determination, but analyses were not yet complete as this paper went to press.

FIT MOUNTAIN TONALITE

Blocky, salmon-orange and grey-weathering, medium-grained tonalite underlies Fit Mountain, and typically contains hornblende and lesser biotite as mafic phases (~35% combined). Medium- to fine-grained quartz and milky white plagioclase account for ~25% and 40% of the rock volume. Fit Mountain tonalite is commonly altered and green-tinged with minor epidote and chlorite veins ranging from millimetres to centimetres in thickness. Magnetite (0.25%) occurs as granular patches, giving the unit a moderately high magnetic susceptibility (~15 SI). Traces of fine-grained lemon-yellow titanite are common. Unlike most parts of the Chilanko intrusive complex, this body is only locally foliated, particularly at the highest elevations on the western side of Fit Mountain. On the eastern side, an area of chlorite-magnetite alteration contains veins of chalcocopyrite and bornite (*see* 'Mineralization' below).

QUARTZ-FIRST GRANODIORITE

Blocky or tabular, white-pink and tan-weathering granodiorite is light yellow-green on fresh surfaces due to pervasive chloritization of mafic minerals and sericitization of feldspars. It is characteristically quartz porphyritic and holocrystalline, with medium-grained quartz, feldspar and biotite intergrown between coarse knots of grey quartz (Figure 13). Both strongly foliated and nonfoliated variants are common within the southeastern Chilanko Forks map area.

Eocene Tatla Lake Stock

North of Tatla Lake, a widely jointed biotite granodiorite stock weathers into rounded, light grey to tan blocks and appears light grey to nearly white on fresh surfaces. Originally mapped by Friedman (1988), who obtained from it an isotopic age of 47.5 Ma, the stock cuts, and is chilled against, strongly foliated granodiorite of the Tatla Lake Metamorphic Complex. It is not foliated.

Tatla Lake stock is medium-grained and subhedral holocrystalline, and contains minor biotite (3–7%) and smoky quartz (35%). Myrmekitic intergrowths of interstitial quartz and potassium feldspar are common. Very minor alteration is limited to rare replacement of biotite by chlorite, and slight turbidity in plagioclase due to secondary white mica. Accessory phases include euhedral titanite and sparse rutile.

GEOCHRONOLOGY

In the Chezacut area, three ~1 km² intrusive bodies were mapped and sampled for geochronological age determination by Mihalyuk et al. (2008a, b). One of these, the

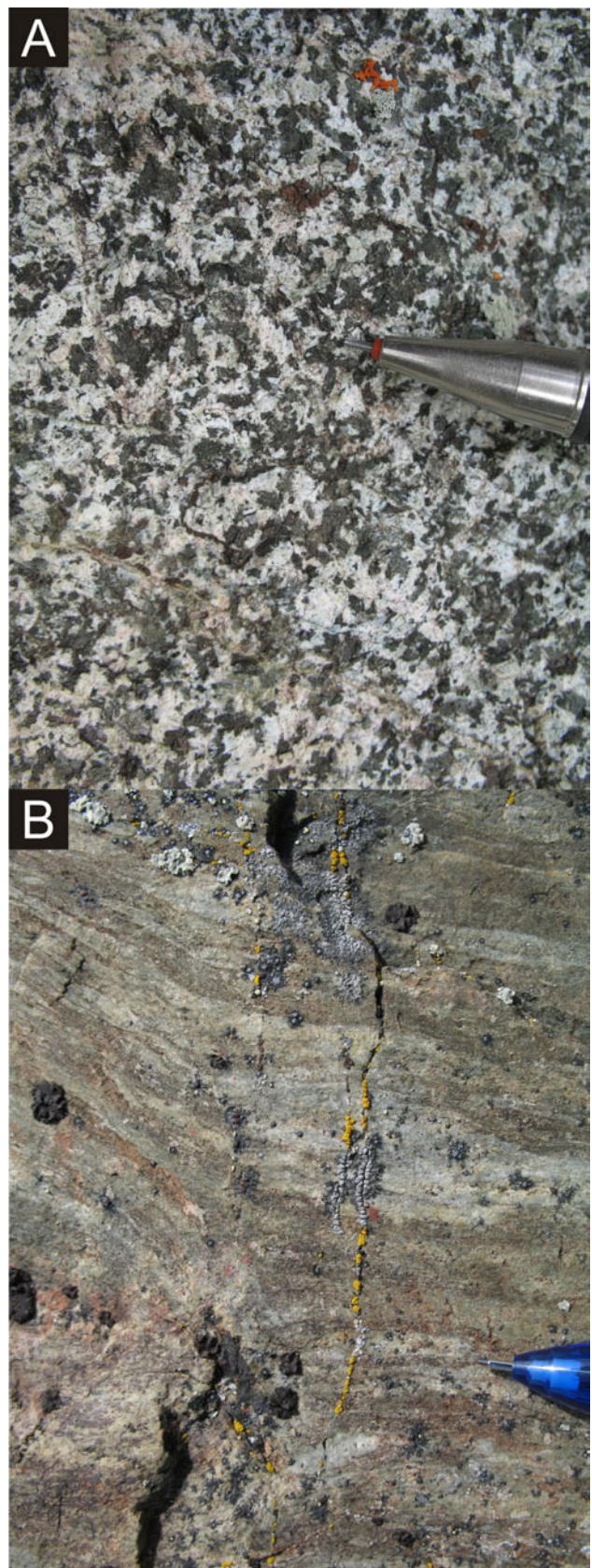


Figure 12. a) Nonfoliated quartz diorite phase within the Chilanko intrusive complex. b) Foliated calcareous country rocks adjacent to the contact of the complex.

Chili dacite stock, is of Eocene age; the other two, the Puntzi Ridge quartz monzonite and the 'Sweetwater Lake' monzonite (Figure 2) are of Late Jurassic age. We report on the geochronological age data from these two older intrusions.

All sample preparation and analytical work for the U-Pb and $^{40}\text{Ar}/^{39}\text{Ar}$ isotopic ages presented here was conducted at the Pacific Centre for Isotopic and Geochemical Research (PCIGR) at the Department of Earth and Ocean Sciences, University of British Columbia.

U-Pb isotopic age determinations reported here (Table 1) are from data acquired by Thermal Ionization Mass Spectrometry (U-Pb TIMS). Argon-40/argon-39 isotopic age determinations are from data acquired by the laser-induced step-heating technique (Table 2). Details of both analytical techniques are presented in Logan et al. (2007).

Sample Descriptions

Samples collected for isotopic age determination are from southeastern and northwestern Chezacut map area. A grapefruit-sized sample was collected from the southeastern pluton, the Puntzi Ridge quartz monzonite (sample site MMI07-45-1, Table 2, Figure 2). The medium-grained, orange, porphyritic monzonite body was sampled at this site (Figure 14a) because it contains vitreous black biotite (5%) and hornblende (15%) an unusual occurrence as both minerals are normally dull green and turbid due to alteration. Accessory minerals include magnetite (~5%), pyrite (~0.25%) and traces of chalcopyrite. Outcrops near the sample site are cut by millimetre-thick sheeted K-feldspar and epidote veins.

Pink, medium-grained, holocrystalline monzonite is the main rock type within the northwestern intrusive body, the 'Sweetwater Lake' monzonite. It contains 3–4% interstitial quartz (locally up to 10%), ~45% K-feldspar, 40% plagioclase, 10% hornblende and 5% biotite. However, pervasive epidote and chlorite alteration attacks calcic cores of plagioclase and renders identification of the mafic minerals difficult. It was necessary to collect a ~20 kg sample from which a sufficient volume of zircons could be extracted (sample site MMI07-48-6, Figure 2).



Figure 13. Quartz-first granodiorite shows typical early porphyritic knots of quartz within a holocrystalline matrix.

U-Pb Protolith Age

Zircon was separated from an approximately 20 kg sample of monzonite using a standard mineral separation technique, which includes crushing, grinding, Wilfley (wet shaker) table, heavy liquids and magnetic separation, followed by hand picking. Eight air abraded single grains selected for analysis were processed using techniques reported in Logan et al. (2007). One of these grains was lost during processing prior to mass spectrometry and two gave weak or unstable signals that did not yield usable data. Analytical results from the remaining five grains are listed in Table 1 and plotted in Figure 15. All data overlap concordia at the 2 σ confidence level (Figure 15a), with the five-point weighted average of overlapping ^{206}Pb - ^{238}U dates at 160.94 \pm 0.13 Ma (Figure 15b) taken as the best estimate for the age of the rock.

$^{40}\text{Ar}/^{39}\text{Ar}$ Cooling Age

Both biotite and hornblende were separated from sample MMI07-45-1. The biotite separate yielded a humped-

Table 1. U-Pb TIMS analytical data for zircon from 'Sweetwater Lake' monzonite.

Grain ¹	Wt ² (mg)	U ³ (ppm)	Pb ⁴ (ppm)	$^{206}\text{Pb}^5$ ^{204}Pb	$^{207}\text{Pb}^6$ ^{206}Pb	Pb ⁷ (pg)	Th/U ⁸	Isotopic ratios $\pm 1\sigma, \%$ ⁹			corr. coef.	% ¹⁰ discordant	Apparent ages $\pm 2\sigma, \text{Ma}$ ¹¹		
								$^{206}\text{Pb}/^{238}\text{U}$	$^{207}\text{Pb}/^{235}\text{U}$	$^{207}\text{Pb}/^{206}\text{Pb}$			$^{206}\text{Pb}/^{238}\text{U}$	$^{207}\text{Pb}/^{235}\text{U}$	$^{207}\text{Pb}/^{206}\text{Pb}$
Sample MMI07-48-6															
B	5.2	436.0	11.6	3992	69.4	0.9	0.599	0.02530 \pm 0.10	0.1719 \pm 0.2	0.04928 \pm 0.15	0.599	0.0	161.1 \pm 0	161.1 \pm 1	161.1 \pm 7.2/7.2
D	7.0	798.0	23.2	12620	233.2	0.7	0.886	0.02532 \pm 0.15	0.1724 \pm 0.2	0.04939 \pm 0.10	0.801	3.3	161.2 \pm 0	161.5 \pm 1	166.6 \pm 4.8/4.8
F	7.3	547.0	14.6	6564	111.1	1.0	0.563	0.02526 \pm 0.19	0.1716 \pm 0.2	0.04927 \pm 0.15	0.765	-0.2	160.8 \pm 1	160.8 \pm 1	160.5 \pm 7.0/7.1
G	5.5	1484.0	43.0	14590	267.1	0.9	0.888	0.02525 \pm 0.08	0.1717 \pm 0.1	0.04932 \pm 0.06	0.859	1.3	160.8 \pm 0	160.9 \pm 0	162.8 \pm 3.0/3.0
H	4.4	843.0	24.4	10800	200.2	0.5	0.725	0.02529 \pm 0.07	0.1720 \pm 0.1	0.04932 \pm 0.11	0.725	1.2	161.0 \pm 0	161.1 \pm 0	163.0 \pm 5.1/5.2

¹All single grains, air abraded.

²Grain mass determined on Sartorius SE2 ultra-microbalance to ± 0.1 microgram.

³Corrected for spike, blank (0.2 pg $\pm 50\%$, 2 σ), and mass fractionation, which is directly determined with ^{233}U - ^{235}U spike.

⁴Radiogenic Pb; data corrected for spike, fractionation, blank and initial common Pb; mass fractionation correction of 0.23% /amu $\pm 40\%$ (2 σ) is based on analysis of NBS-982 throughout course of study; blank Pb correction of 0.5-0.9 pg $\pm 40\%$ (2 sigma) with composition of $^{206}\text{Pb}/^{204}\text{Pb} = 18.5 \pm 2\%$, $^{207}\text{Pb}/^{204}\text{Pb} = 15.5 \pm 2\%$, $^{208}\text{Pb}/^{204}\text{Pb} = 36.4 \pm 2\%$, all at 2 σ ; initial common Pb compositions based on Stacey and Kramers (1975) model Pb at the interpreted age of the rock.

⁵Measured ratio corrected for spike and fractionation.

⁶Ratio of radiogenic to common Pb.

⁷Total weight of common Pb calculated with blank isotopic composition.

⁸Model Th/U ratio calculated from radiogenic $^{207}\text{Pb}/^{206}\text{Pb}$ ratio and $^{207}\text{Pb}/^{206}\text{Pb}$ age.

⁹Corrected for spike, fractionation, blank and initial common Pb.

¹⁰Discordance in % to origin.

¹¹Age calculations are based on decay constants of Jaffey et al. (1971).

Table 2. Ar isotopic data from Puntzi Ridge quartz monzonite.

Laser Power(%)	Isotope Ratios $^{40}\text{Ar}/^{39}\text{Ar}$	$^{38}\text{Ar}/^{39}\text{Ar}$	$^{37}\text{Ar}/^{39}\text{Ar}$	$^{36}\text{Ar}/^{39}\text{Ar}$	Ca/K	Cl/K	$\%^{40}\text{Ar atm f}^{39}\text{Ar}$	$^{40}\text{Ar}/^{39}\text{ArK}$	Age	
Sample MMI07-45-1										
2	115.2233 ± 0.0055	1.4680 ± 0.0111	4.4609 ± 0.0167	0.3364 ± 0.0175	15.3	0.322	85.82	17.1	16.330 ± 1.724	145.43 ± 14.75
2.2	283.1358 ± 0.0941	0.3750 ± 0.4352	1.8510 ± 1.5255	0.8857 ± 0.1339	6.043	0.04	88.65	0.12	25.512 ± 26.303	222.34 ± 215.67
2.4	111.6997 ± 0.0503	0.4008 ± 0.1464	0.5939 ± 1.0879	0.3098 ± 0.0712	1.934	0.074	76.98	0.36	21.394 ± 5.056	188.26 ± 42.25
2.7	75.2856 ± 0.0215	0.2663 ± 0.0507	1.0841 ± 0.8500	0.1936 ± 0.0556	3.678	0.049	73.67	1.33	18.459 ± 2.989	163.56 ± 25.32
3	41.1631 ± 0.0127	0.1311 ± 0.0354	0.6036 ± 0.3130	0.0810 ± 0.0396	2.09	0.023	55.16	2.97	17.398 ± 0.938	154.55 ± 7.99
3.3	29.4392 ± 0.0075	0.2237 ± 0.0480	1.2511 ± 0.2216	0.0418 ± 0.0504	4.354	0.046	38.53	5.5	17.319 ± 0.636	153.88 ± 5.41
3.6	26.7454 ± 0.0064	0.4487 ± 0.0188	2.2229 ± 0.0844	0.0337 ± 0.0370	7.752	0.099	33.89	8.74	17.172 ± 0.386	152.62 ± 3.29
4	22.4389 ± 0.0047	1.9552 ± 0.0095	5.4533 ± 0.0142	0.0198 ± 0.0222	19.11	0.45	21.26	29.2	17.568 ± 0.158	155.99 ± 1.34
4.3	20.9618 ± 0.0063	1.6863 ± 0.0139	4.5753 ± 0.0276	0.0146 ± 0.0587	16.01	0.387	14.83	13.2	17.475 ± 0.280	155.21 ± 2.39
4.6	19.9892 ± 0.0074	1.3166 ± 0.0177	3.5043 ± 0.0155	0.0111 ± 0.0582	12.25	0.301	10.86	12.1	17.352 ± 0.236	154.16 ± 2.01
4.9	20.0264 ± 0.0128	0.3988 ± 0.0290	1.4738 ± 0.0565	0.0112 ± 0.0929	5.176	0.088	11.84	9.35	17.002 ± 0.383	151.17 ± 3.26
Total/Average	39.4907 ± 0.0013	1.3023 ± 0.0028	7.2375 ± 0.0031	0.0775 ± 0.0067	13.31	0.171			100	17.246 ± 0.160

J = 0.005141 ± 0.000012

Volume ^{39}ArK = 96.16

Integrated Date = 153.25 ± 2.75

Volumes are 1E^{13} cm³ NPT

Neutron flux monitors: 28.02 Ma FCs (Renne et al., 1998)

Isotope production ratios: ($^{38}\text{Ar}/^{39}\text{Ar}$)K=0.0302 ± 0.00006, ($^{37}\text{Ar}/^{39}\text{Ar}$)Ca=1416.4 ± 0.5, ($^{36}\text{Ar}/^{39}\text{Ar}$)Ca=0.3952 ± 0.0004,

Ca/K=1.83 ± 0.01 ($^{37}\text{ArCa}/^{39}\text{ArK}$).

shaped release spectrum with no reliable plateau age, suggesting the presence of excess argon. In addition, the computed inverse isochron ages are not reasonable. The best age estimate that can be obtained from the biotite data is the integrated plateau age of 155.9 ± 0.5 , but this is suspect and made redundant with a well-behaved hornblende separate. The hornblende plateau age of 155.1 ± 1.2 Ma represents

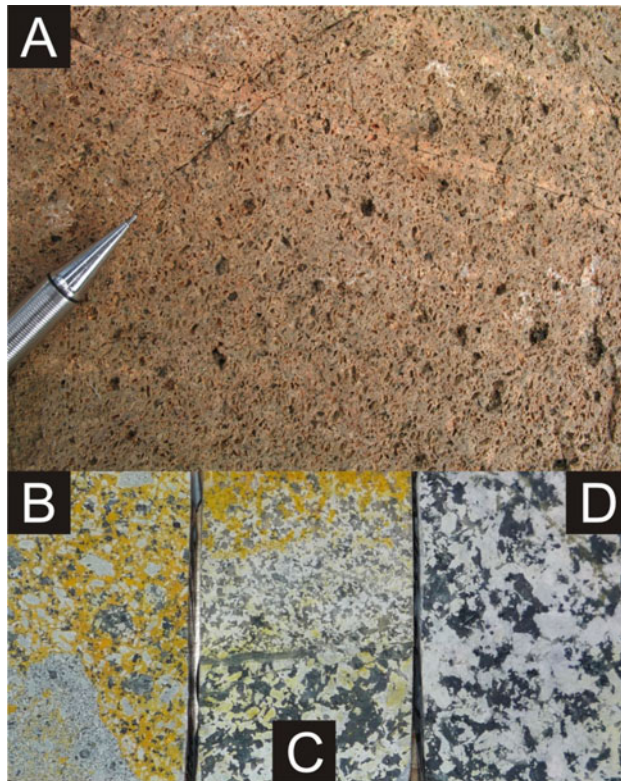


Figure 14. a) Typical exposure of Puntzi Ridge quartz monzonite and b) thin section cut-off with yellow-stained K-feldspar from a high-level tuffaceous equivalent of the monzonite. c) Chilanko Igneous Complex quartz diorite with finer-grained, crosscutting monzogranite dike and d) unaltered quartz diorite of the complex.

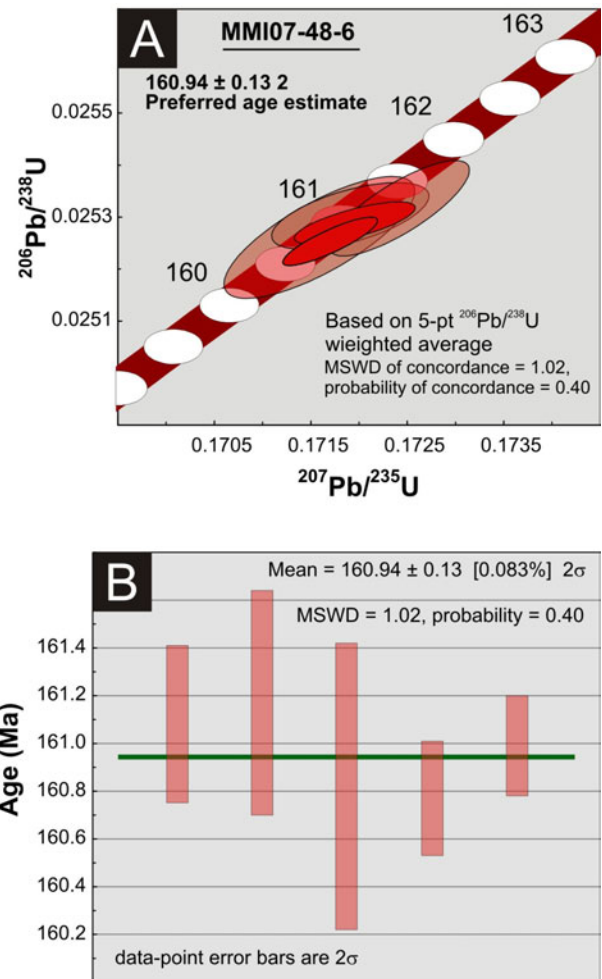


Figure 15. a) Concordia plots for U-Pb TIMS data for sample MMI07-48-6. The 2 σ error ellipses for individual analytical fractions are in red. Concordia bands include 2 σ errors on U decay constants. b) Mean square weighted deviates (MSWD) plot for the five fractions. Box heights are 2 σ .

90.7% of the ^{39}Ar released (Figure 16a, only the highest temperature step is omitted). The age is confirmed by an inverse isochron model age for the six high temperature steps which yields 154.4 ± 2.9 Ma (Figure 16b).

Implications of Geochronology

Polyphase, variably foliated dioritic parts of the northern ‘Sweetwater Lake’ monzonite intrusion are very similar to parts of the Chilanko intrusive complex, which underlies much of the southeastern Chilanko Forks area (Figure 2). Penetrative fabrics are lacking within the main ‘Sweetwater Lake’ monzonitic body. Similarly, undeformed monzonitic phases are seen to cut the more foliated parts of the Chilanko intrusive complex (Figure 14c). If this correlation is correct, a relative age relationship is demonstrated, consistent with the isotopic ages reported here.

Mihalynuk et al. (2008b) suggested that although the Puntzi Ridge quartz monzonite cuts structurally lower Mesozoic arc strata, it may be comagmatic with some of the younger Mesozoic tuffaceous rocks (Figure 14b).

An implication of the foregoing inferences is that both the growth of the middle arc succession and deformation affecting the Chilanko intrusive complex are bracketed at between ~161 and ~152 Ma. This deformation age is consistent with syndeformational fabrics within the complex (see next section), and appears coeval with deformation in southwest Anahim Lake map area (van der Heyden, 2004).

STRUCTURE AND DEFORMATION

Youngest rocks within the region, those of the Oligocene-Pleistocene Chilcotin Group and/or Pleistocene-Holocene Anahim volcanic belt, are not folded. However, Mihalynuk et al. (2008b) showed that even the youngest rocks appear to be cut by high angle reverse faults. No evidence of such deformation was observed in the sparse exposures of these rocks within the Chilanko Forks or Klusko River areas.

Pervasive deformational fabrics were probably formed in Late Jurassic, mid-Cretaceous and Early Eocene times. At least two stages of deformation have affected Mesozoic rocks, including Late Jurassic rocks within the Tatla Lake Metamorphic Complex (Friedman, 1988) and probable correlative rocks deformed at a higher crustal level (Mihalynuk and Friedman, 2009) and now included within the informally named Chilanko intrusive complex. In contrast, the Eocene Ootsa Lake Group displays only locally developed cleavage.

Jurassic Deformation

Jurassic deformation is indicated by the syndeformational intrusive fabrics preserved within the Chilanko intrusive complex. Such fabrics include crosscutting of foliated intrusive phases by phases that appear compositionally identical, but which are weakly to nonfoliated. If the Klusko Intrusive Complex is dated at ~161–152 Ma, as argued above, then synemplacement metamorphism is broadly correlative with that within the Atnarko Crystalline Complex (western part of NTS 093C). The U-Pb metamorphic ages of those rocks are interpreted as 158.8 ± 0.3 Ma and 157 ± 11 Ma, based on metamorphic zircon from ductilely sheared metarhyolite, and syn- to late-kinematic quartz diorite (van der Heyden, 2004), respectively. These

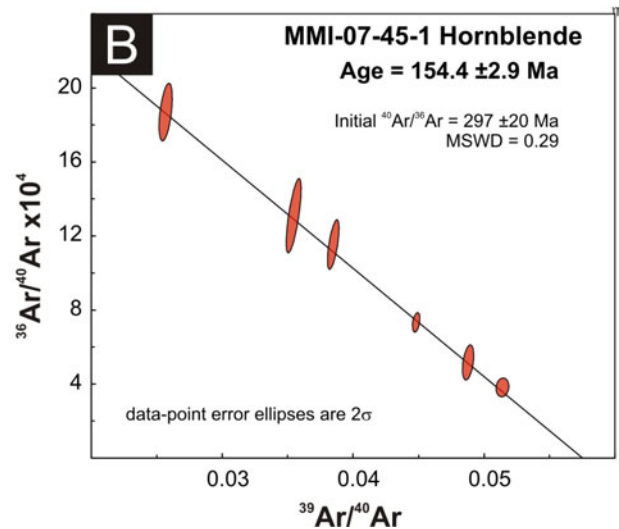
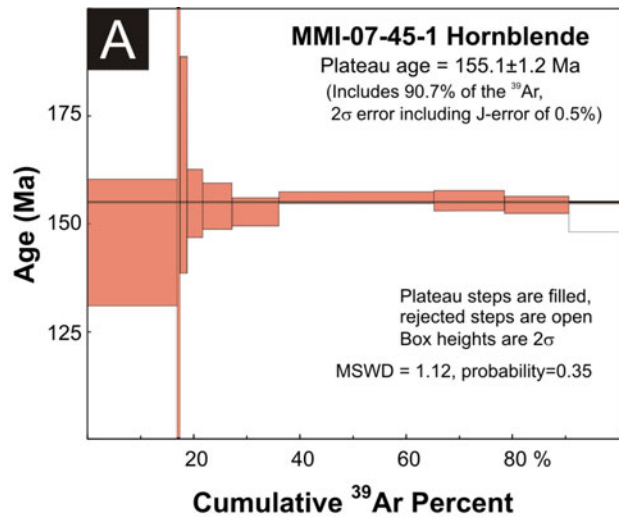


Figure 16. a) Step heating Ar gas release spectra for hornblende sample MMI07-45-1. Filled plateau steps produce an age of 155.1 ± 1.2 Ma (90.7% of ^{39}Ar , rejected step is open). Box heights at each step are 2σ . **b)** The Ar isotope ratio correlation plots for plateau steps in a) provide a reliable age determination of 154.4 ± 2.9 Ma, identical within error to the plateau age.

ages span the Middle–Upper Jurassic boundary of 156.6 ± 2.0 – 2.7 Ma (Pálffy et al., 2000).

Late Eocene-Oligocene Deformation

Broad folds are interpreted to deform the Ootsa Lake Group with production of local, open parasitic folds and axial cleavage. This cleavage is well developed only locally, but in such localities it is obvious, causing platy segmentation of outcrops with folia passing through clasts. Such fabric should not be confused with much more common flow foliation that also results in platy parting, but does not pass through fragments or clasts contained within the flows. Axial cleavage is best developed 4 km southeast of Thunder Mountain, along strike of the Mesozoic uplift and fold hinge mapped in the Chezacut area (Mihalynuk et al., 2008a). Another fold mapped by Mihalynuk et al. (2008a), about 8 km farther west, could not be verified by mapping

along strike to the north. It may not exist, as in the reinterpretation offered in Figure 2, or it may die out as it passes from the southern to the northern part of the Chezacut map area. In most other parts of the Clusko River area, tilting of Eocene strata is probably due to block faulting.

The age of deformation of the Ootsa Group has not been conclusively constrained. However, the tendency of the upper, younger units (~46–44 Ma, see ‘Ootsa Lake Group’ above) to lie flat (Figure 9e) while the underlying rocks (~54–50 Ma) are moderately tilted, suggests an intervening period of deformation. This age of deformation is consistent with a rapid regional cooling at ~50 Ma, as determined from fission tracks (Riddell and Ferri, 2008) and extensional faulting in the nearby Tatla Lake Metamorphic Complex between 55 ± 3 and 47 ± 1.5 Ma (Friedman, 1988), which is herein postulated to extend to southeastern Chilanko Forks area; see also Mihalynuk et al., 2009) where deformed Jurassic rocks are widely affected by block faulting.

Beautifully corrugated and polished fault planes (Figure 17) have a spacing of ~5–10 m within intermittently exposed, ductilely deformed Chilanko intrusive complex rocks in the southeastern corner of NTS 093C/01. Fault planes are lined with comminuted quartz and epidote, dip moderately east and generally display normal to slightly oblique offsets (although overprinted fault plane fabrics with reverse offset are not uncommon). These faults cut an earlier shallow, intense mylonite fabric (Figure 18a) and subhorizontal west-trending folds. Mylonite is overprinted by sets of centimetre-scale, domino-style normal faults (Figure 18b); with increasing downdip offset on these normal faults, the mylonite becomes brecciated (Figure 18c). The breccia consists of cemented quartz and chlorite. We tentatively interpret the brecciation as recording a ductile to brittle transition at a detachment fault. The corrugated, moderately east-dipping normal faults are antithetic with respect to top-to-the-west motion documented on extensional shear zones of the Tatla Lake Metamorphic Complex (Friedman, 1988) and are typical of early brittle shears within the brittle-ductile transition zone footwall of detachment faults (e.g., Sacramento Mountains core complex; Stewart and Argent, 2000). Locally derived clastic rocks atop the sheared intrusive rocks are likely deposited in small synextensional basins within a few hundred verti-



Figure 17. Moderately east-dipping, beautifully corrugated and polished brittle fault plane.

cal metres of the detachment surface. Unlike the main detachment fault, which exhumes high grade rocks in the core of the Tatla Lake Metamorphic Complex, the detachment fault mapped within the southeast portion of the Chilanko Forks map area is a relatively minor structure and shows little evidence of major crustal omission across it.

Middle to upper amphibolite-grade lower plate rocks of the Tatla Lake Metamorphic Complex are separated from greenschist-grade upper plate rocks by a 1–2.5 km thick ‘ductilely sheared assemblage’ (DSA; Friedman,

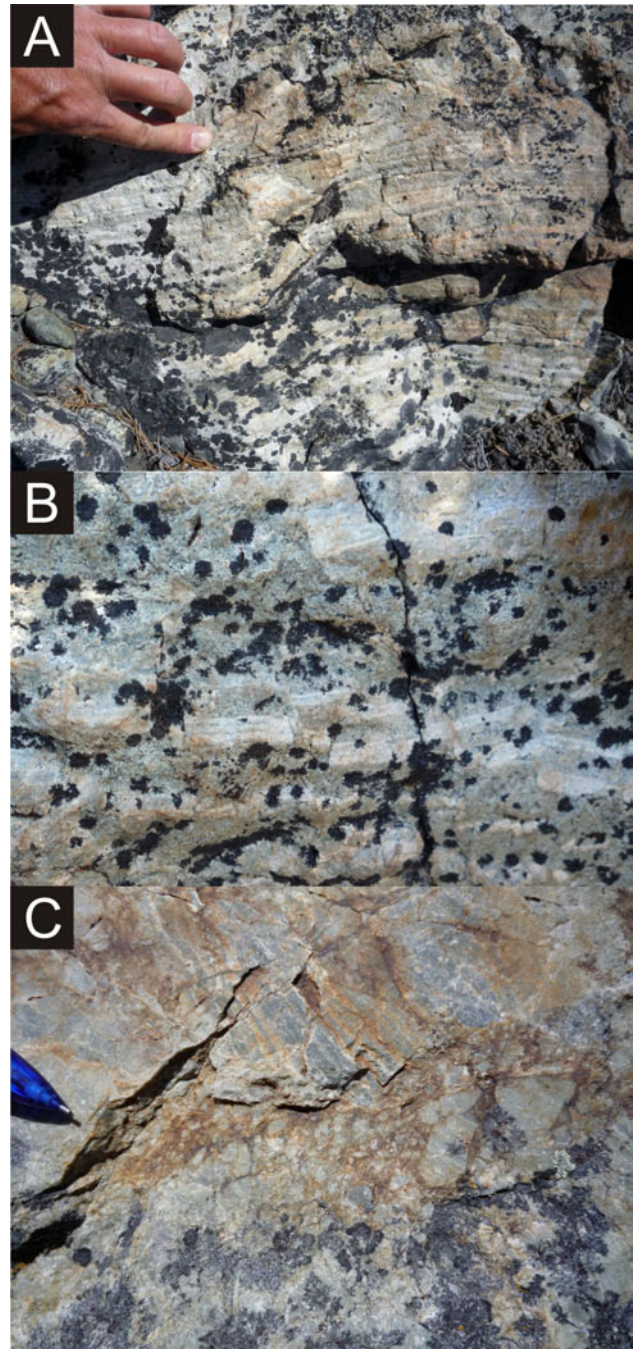


Figure 18. a) Well-developed mylonitic fabric locally includes ptzygmatic veins. b) Domino-style brittle faults cutting the mylonitic fabric. c) Increased offset on brittle faults produces disaggregated and recemented breccia.

1988). Within the Chilanko Forks area, rocks belonging to the DSA crop out north and south of Takla Lake. To the north, they consist of strongly foliated biotite granodiorite and, to the south, they are strongly foliated and lineated green schistose rocks, probably former volcanoclastic strata.

MINERALIZATION

Within the Chilanko Forks area and southern half of the Clusko River area, only two mineral occurrences are recorded in MINFILE: ‘Chilcotin River East’ (MINFILE 093C 014) and ‘Chilcotin River West’ (MINFILE 093C 013). Both of these “consist...of copper mineralization within...Ootsa Lake Group intermediate to felsic volcanic and related rocks” (MINFILE, 2007) north of the Chilcotin River in NTS 093C/09S. Neither showing was encountered during the course of our mapping. Within the intervening Chezacut map area, several new mineral occurrences were discovered by Mihalynuk et al. (2008b).

Newmac Resources Inc. is owner and operator of the CA prospect (Chilanko River property), located just 6 km west of the southern Chilanko Forks map area. Here mineralization consists of disseminated chalcocopyrite within a locally foliated quartz diorite-andesite dike complex (Fleming, 1996) that is almost certainly correlative with the Chilanko intrusive complex. Within, or adjacent to the Chilanko complex, three copper showings were found during the course of mapping in the 2008 field season: the Fit, ET and Ejewra showings (see Table 3 and Figure 2 for locations). Scattered angular sericite-altered float displaying an epithermal geochemical signature was also found adjacent to the complex. North of Tatla Lake, intrafolial chalcocopyrite and malachite were found within a ~3.5 m³ erratic of gneissic granodiorite. North of Chilanko River, a sample of altered Eocene tuff returned elevated As and Au (INAA: 18 ppm, 83 ppb). Analyses of grab samples obtained from these showings are listed in Table 3.

Fit Showing

Minor copper-silver mineralization is found in scattered tonalite outcrops and angular boulders over a ~50 m² area about 0.75 km northeast of Fit Mountain summit. Mineralization within the intrusion accompanies chlorite-magnetite alteration. It consists of veinlets and disseminations

of chalcocopyrite and subordinate bornite together with epidote-magnetite-chlorite-quartz-calcite veining (Figure 19a, b) and matrix replacement. Analyses of samples collected returned up to 0.18% Cu, 2.2 g/t Ag, and 20 ppb Au (MMI08-6-3, Table 3). Attempts to track the mineralized zone beyond the local outcrops were not successful, although mineralization crops out ~1.2 km to the northwest in the thermal-metamorphic halo of the Fit Mountain tonalite. Within the contact zone, strongly altered (chlorite-calcite±epidote±albite+scapolite (?)) and brecciated outcrop is exposed over a ~10 m² area. A grab sample of the altered and mineralized breccia returned 0.37% Cu, 2.87 g/t Ag and 63 ppb Au.

Ejewra Showing

A grab sample collected approximately 4 km southeast of Fit Mountain (EOR08-13-3, Table 3) returned 0.58% Cu, 4.2 g/t Ag and 40 ppb Au. A large angular block (probable erratic) 1.1 km to the northwest contained more than 10% pyrite and a grab sample collected from it contained 7.47 g/t Te (and lesser concentrations of the above noted elements). It is worthwhile noting that the probable erratic is up-ice of the outcrop sample and must be derived from a separate mineralized zone (or one that is continuous for over 1 km).

ET Showing

About 2.5 km northeast of Pyper Lake and 0.8 km west of the Chilanko igneous complex contact, variably foliated tuffaceous rocks (Figure 19c) contain veins of quartz-calcite (±rhodochrosite)-epidote-chlorite±chalcocite and malachite, which make up the ET showing (Figure 2). Veins up to 15 cm thick contain irregular knots of chalcocite up to 2 cm across. Grab samples collected from various veins contain up to 0.12% Cu, 2.8 g/t Ag and 0.2 g/t Au (Table 3).

Abundant, fist-sized, angular, rusty float is scattered over several square metres of hillside ~1.8 km south of the ET showing. Portions of five angular quartz- and sericite-altered clasts were combined and analyzed. Results show elevated base metal values, including 0.4 g/t Ag, 11.9 ppm As, 22 ppm Hg, as well as 84 and 55 ppb Au (via ICP and INAA methods, respectively; MMI08-31-3, Table 3). These results correspond to an epithermal geochemical signature and may warrant further evaluation given the abun-

Table 3. Analytical subset for selected grab samples.

Sample ID	Name	Location	Latitude	Method Longitude	Cu	Pb	Zn	Ag	Au	Te	Hg	As	Zn	Ag	Au	As
					ICP-MS (ppm)	ICP-MS (ppm)	ICP-MS (ppm)	ICP-MS (ppb)	ICP-MS (ppb)	ICP-MS (ppm)	ICP-MS (ppm)	INAA (ppm)	INAA (ppb)	INAA (ppb)	INAA (ppm)	
EOR08-13-3	Ejewra	Fit Mtn. S	52.18	-124.22	5826.64	5.84	170.6	4199	40	0.88	85	2.8	<50	<5	44	9.2
EOR08-13-5	Ejewra float	Fit Mtn. S	52.19	-124.23	99.02	3.91	61.7	101	7	7.47	<5	4.3	<50	<5	<2	6.0
MMI08-2-2	no name: float	Fit Mtn. S	52.16	-124.25	8.69	0.94	20.5	45	<0.2	0.80	309	1.0	<50	<5	<2	4.8
MMI08-5-1	Chili	Chezacut SE	52.31	-124.03	1473.66	23.84	195.5	13186	93	4.42	<5	17.0	230	23	120	34.2
MMI08-5-1rep	Chili	Chezacut SE	52.31	-124.03	1565.99	24.51	188.3	14477	101	4.80	<5	15.8	240	24	120	35.4
MMI08-6-3	Fit	Fit Mtn	52.21	-124.24	1861.30	7.02	95.1	2226	20	0.17	<5	1.9	<50	<5	27	5.9
MMI08-6-8B	Fit	Fit Mtn	52.22	-124.25	3707.11	10.25	57.5	2872	63	0.19	7	0.7	<50	<5	<2	9.5
MMI08-13-7	no name	Chilanko R. N	52.12	-124.40	28.99	2.73	44.4	10	<0.2	<0.02	<5	0.5	<50	<5	83	18.0
MMI08-31-3	no name	Pyper Lk. E	52.05	-124.13	131.77	42.12	52.8	443	84	4.37	22	11.9	<50	<5	55	2.7
MMI08-31-12	ET	Pyper Lk. NE	52.07	-124.14	1152.92	1.42	14.2	853	15	<0.02	<5	<0.1	<50	<5	29	1.0
MMI08-31-12rep	ET	Pyper Lk. NE	52.07	-124.14	1214.07	1.39	13.3	987	202	0.03	5	<0.1	<50	<5	29	1.0
MMI08-41-6	Erratic	Tatla Lk N of E	52.02	-124.37	4040.24	1.61	10.5	2465	11	0.12	<5	1.1	<50	<5	8	3.0
TBA08-38-4	ET	Pyper Lk.	52.03	-124.04	1276.51	51.22	246.4	2857	2	0.26	5	0.9	260	<5	<2	4.0
Detection limit					0.01	0.01	0.1	2	1	0.02	5	0.1	50	5	2	0.5

Notes: INAA, instrumental neutron activation analysis; ICP-MS, inductively coupled plasma mass spectrometry
A full list of samples and elements analyzed can be obtained for both INAA and ICP-MS suites from
http://www.em.gov.bc.ca/Mining/GeolSurv/Publications/catalogue/cat_geof.htm

dance and angularity of the clasts, which suggest a nearby source.

Erratic

North of eastern Tatla Lake an erratic of foliated granodiorite contains intrafolial chalcopyrite-malachite and tetrahedrite(?). One grab sample yielded 0.4% Cu and 2.4 g/t Ag. Mineralization is confined to one ~20 cm thick

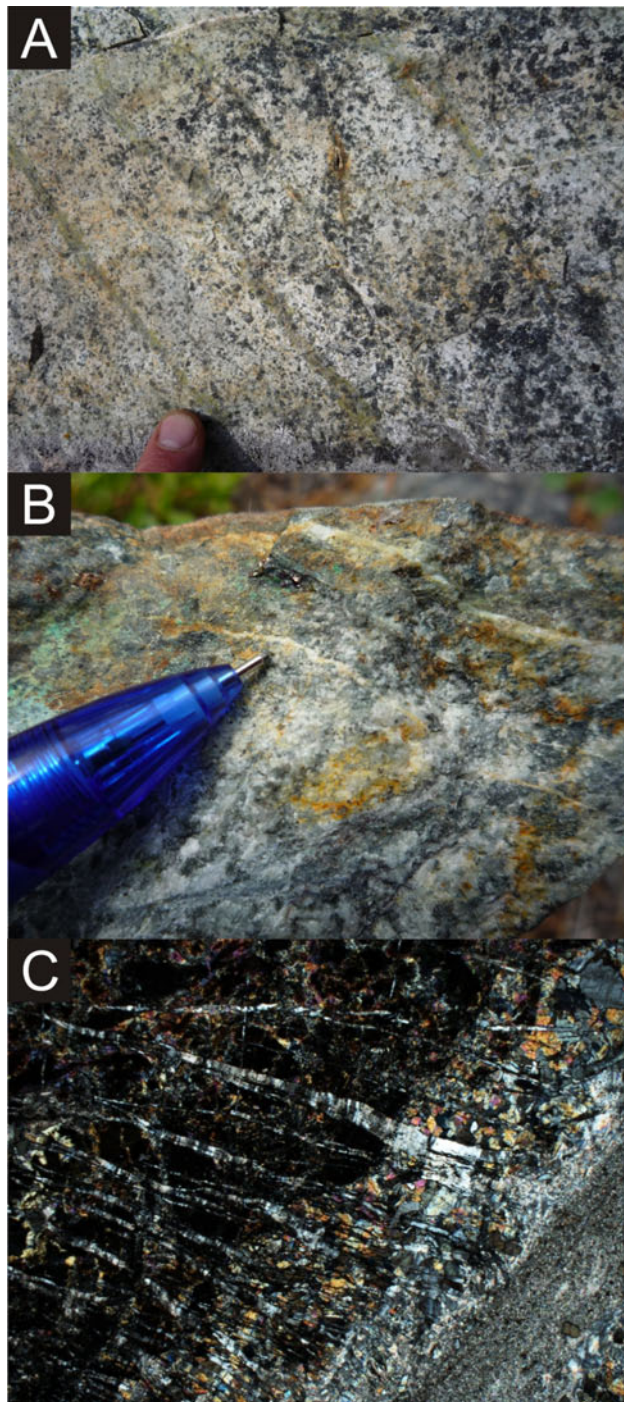


Figure 19. a) Sheeted veins within Fit Mountain tonalite. b) Veinlets contain chalcopyrite and bornite. c) Abundant calcite veinlets within foliation in epidotized tuff near the ET showing.

foliaform zone (Figure 20). Even though this large (~3.5 m³) erratic lies within 100 m of outcrop, a thorough search of the surrounding ~1 km² did not reveal any mineralized bedrock or other mineralized erratics.

Regional Mineral Potential

Some hints of epithermal mineralization within the Eocene Ootsa Lake Group were revealed by analysis of altered tuffs from north of the Chilanko River and from quartz- and sericite-altered float south of the ET showing. However, if the frequency of discovery during our 2008 field mapping in the Chilanko Forks area (NTS 093C/01) can be used as an indicator, the greatest potential for future discoveries lies within the Chilanko intrusive complex. Our findings are confirmed by the work of Newmac Resources Inc. and predecessors at the Chilanko property in adjacent parts of NTS 093C/02. Thus, this >330 km² complex, together with rocks in the adjacent thermal metamorphic halo, warrants further systematic exploration.

ACKNOWLEDGMENTS

T. Ullrich processed the ⁴⁰Ar/³⁹Ar samples and generated the step release data, spectra and inverse isochron plots. J. Riddell offered peer review of this paper. P. Metcalfe is thanked for his candid discussions with regards to former data density in the southern Clusko map area. R. Lett provided rock solid reliability in the delivery of geochemical data with fine quality control for this and past unacknowledged years. Assistance with mineral separation and mass spectrometry was provided by H. Lin and Y. Feng helped with grain selection, pre-treatment and sample dissolution/processing. J. Wardle was always close at hand to lend assistance in the field. M. and A. McMath were tremendously accommodating hosts at our Puntzi Lake base camp.



Figure 20. Erratic of strongly foliated granodiorite contains a 20 cm thick foliaform zone of malachite+tetrahedrite (?).

REFERENCES

Alfaro, R., Campbell, R., Vera, P., Hawkes, B. and Shore, T. (2004): Dendroecological reconstruction of mountain pine beetle outbreaks in the Chilcotin Plateau of British Columbia; in Mountain Pine Beetle Symposium: Challenges and

- Solutions, T.L. Shore, J.E. Brooks and J.E. Stone, Editors, *Natural Resources Canada*, Canadian Forest Service, Pacific Forestry Centre, Information Report BC-X-399, pages 245–256.
- Andrews, G.D.M. and Russell, J.K. (2007): Mineral exploration potential beneath the Chilcotin Group (NTS 0920, P, 093A, B, C, F, G, I, J, K), south-central British Columbia: preliminary insights from volcanic facies analysis; in *Geological Fieldwork 2006, BC Ministry of Energy, Mines and Petroleum Resources*, Paper 2007-1 and Geoscience BC, Report 2007-1, pages 229–238.
- BC Ministry of Forests and Range (2005a): The state of British Columbia's forests 2004; *BC Ministry of Forests and Range*, URL <<http://www.for.gov.bc.ca/hfp/sof/2004/>> [November 2007].
- BC Ministry of Forests and Range (2005b): British Columbia's Mountain Pine Beetle Action Plan 2005-2010; *Government of British Columbia*, 20 pages, URL <http://www.for.gov.bc.ca/hfp/mountain_pine_beetle/actionplan/2005/actionplan.pdf> [October 2, 2006].
- BC Ministry of Forests and Range (2008): About Us; *BC Ministry of Forests and Range*, URL <<http://bcwildfire.ca/AboutUs/>> [October 2008].
- Bevier, M.L. (1983): Regional stratigraphy and age of Chilcotin Group basalts, south-central British Columbia; *Canadian Journal of Earth Sciences*, Volume 20, pages 515–524.
- Bevier, M.L. (1989): A lead and strontium isotopic study of the Anahim volcanic belt, British Columbia: additional evidence for widespread suboceanic mantle beneath western North America; *Geological Society of America Bulletin*, Volume 101, pages 973–981.
- Cassidy, J. and Al-Khoubbi, I. (2007): A passive seismic investigation of the geological structure within the Nechako Basin; in *The Nechako Initiative-Geoscience Update, BC Ministry of Energy, Mines and Petroleum Resources*, Petroleum Geology Open File 2007-1, pages 7–57, URL <http://www.empr.gov.bc.ca/OG/oilandgas/petroleumgeology/ConventionalOilAndGas/InteriorBasins/Documents/The_Nechako_Initiative-Geoscience_Update_2007.pdf> [November 2008].
- Diakow, L.J. and Barrios, A. (2009): Geology and mineral occurrences of the mid-Cretaceous Spences Bridge Group near Merritt, southern British Columbia (parts of NTS 092H/14, 15, 092I/02, 03); in *Geological Fieldwork 2008, BC Ministry of Energy, Mines and Petroleum Resources*, Paper 2009-1, pages 63–80.
- Diakow, L.J. and Levson, V.M. (1997): Bedrock and surficial geology of the southern Nechako Plateau, central British Columbia; *BC Ministry of Energy, Mines and Petroleum Resources*, Geoscience Map 1997-2, scale 1:100 000.
- Diakow, L.J., Webster, I.C.L., Richards, T.A. and Tipper, H.W. (1997): Geology of the Fawnie and Nechako Ranges, southern Nechako Plateau, central British Columbia (93F/2, 3, 6, 7); in *Interior Plateau Geoscience Project: Summary of Geological, Geochemical and Geophysical Studies*; *BC Ministry of Energy, Mines and Petroleum Resources*, Paper 1997-2, pages 7–30.
- Ferbey, T., Vickers, K.J., Hietava, T.J.O. and Nicholson, S.C. (2009): Quaternary geology and till geochemistry of the Redstone and Loomis Lake map areas, central British Columbia (NTS 93B/04, 05); in *Geological Fieldwork 2008, BC Ministry of Energy, Mines and Petroleum Resources*, Paper 2009-1, pages 117–126.
- Ferri, F. and Riddell, J. (2006): The Nechako Basin project: new insights from the southern Nechako Basin; in *Summary of Activities 2006, BC Ministry of Energy, Mines and Petroleum Resources*, Paper 2007-2, pages 89–124.
- Fleming, D.B. (1996): Chilanko River property; *BC Ministry of Energy, Mines and Petroleum Resources*, Assessment Report 24324, 10 pages (plus appendices and maps), URL <<http://www.em.gov.bc.ca/DL/ArisReports/24324.PDF>> [November 2008].
- Friedman, R.M. (1988): Geology and geochronology of the Eocene Tatla Lake metamorphic core complex, western edge of the Intermontane Belt, British Columbia: Ph.D. thesis, *The University of British Columbia*, 348 pages.
- Friedman, R.M. (1992): P-T-t path for the lower plate of the Eocene Tatla Lake metamorphic core complex, southwestern Intermontane Belt, British Columbia; *Canadian Journal of Earth Sciences*, Volume 29, pages 972–983.
- Friedman, R.M. and Armstrong, R.L. (1988): Tatla Lake Metamorphic Complex: an Eocene metamorphic core complex on the southwestern edge of the Intermontane Belt of British Columbia; *Tectonics*, Volume 7, pages 1141–1166.
- Geological Survey of Canada (1994): Magnetic residual total field, Interior Plateau of British Columbia; *Geological Survey of Canada*, Open File 2785, 19 maps at 1:100 000 and 1:250 000 scale.
- Hayward, N. and Calvert, A. (2008): Structure of the south-eastern Nechako Basin, British Columbia: results of seismic interpretation and first-arrival tomographic inversion; in *Back to Exploration (extended abstract)*, CSPG CSEG CWLS Convention, Calgary, pages 612–616, URL <<http://www.cspg.org/conventions/abstracts/2008abstracts/027.pdf>> [November 2008].
- Holland, S.S. (1964): Landforms of British Columbia; *BC Ministry of Energy, Mines and Petroleum Resources*, Bulletin 48 (revised 1976), 138 pages.
- Jaffey, A.H., Flynn, K.F., Glendenin, L.E., Bentley, W.C. and Essling, A.M. (1971): Precision measurement of half-lives and specific activities of ^{235}U and ^{238}U ; *Physical Review C*, Volume 4, pages 1889–1906.
- Kerr, D.E. and Giles, T.R. (1993): Surficial geology of the Chezacut map area (NTS 93C/8); *BC Ministry of Energy, Mines and Petroleum Resources*, Open File 1993-17, scale 1:50 000.
- Larocque, J.P. and Mihalynuk, M.G. (2009): Geochemical character of Neogene volcanic rocks of the central beetle-infested zone, south-central British Columbia (NTS 093B, C); in *Geological Fieldwork 2008, BC Ministry of Energy, Mines and Petroleum Resources*, Paper 2009-1, pages 109–116.
- LeMaître, R.W., Bateman, P., Dudek, A., Keller, J., Le Bas, M.J., Sabine, P.A., Schmid, R., Sorensen, H., Streckeisen, A., Wooley, A.R. and Zanettin, B. (1989): A Classification of Igneous Rocks and Glossary of Terms; *Blackwell Scientific Publications*, Oxford, United Kingdom, 193 pages.
- Levson, V.M. and Giles, T.R. (1997): Quaternary geology and till geochemistry studies in the Nechako and Fraser plateaus, central British Columbia (NTS 93C/1, 8, 9, 10; F/2, 3, 7; 93L/16; 93M/1); in *Interior Plateau Geoscience Project: Summary of Geological, Geochemical and Geophysical Studies*, L.J. Diakow, P. Metcalfe and J. Newell, Editors, *BC Ministry of Energy, Mines and Petroleum Resources*, Paper 1997-2, pages 121–145.
- Logan, J.M., Mihalynuk, M.G., Ullrich, T. and Friedman, R.M. (2007): U-Pb ages of intrusive rocks and $^{40}\text{Ar}/^{39}\text{Ar}$ plateau ages of copper-gold-silver mineralization associated with alkaline intrusive centres at Mount Polley and the Iron Mask Batholith, southern and central British Columbia; in *Geological Fieldwork 2006, BC Ministry of Energy, Mines and Petroleum Resources*, Paper 2007-1, pages 93–116, URL <<http://www.em.gov.bc.ca/DL/GSBPubs/GeoFldWk/2006/11-Logan.pdf>> [November 2008].
- Massey, N.W.D., MacIntyre, D.G., Desjardins, P.J. and Cooney, R.T. (2005): Digital geology map of British Columbia: whole province; *BC Ministry of Energy, Mines and Petroleum Resources*, GeoFile 2005-1, scale 1:250 000, URL

- <<http://www.empr.gov.bc.ca/Mining/Geoscience/PublicationsCatalogue/GeoFiles/Pages/2005-1.aspx>>.
- Mathews, W.H. (1989): Neogene Chilcotin basalts in south-central British Columbia: geology, ages, and geomorphic history; *Canadian Journal of Earth Sciences*, Volume 26, pages 969–982.
- Metcalfe, P., Richards, T.A., Villeneuve, M.E., White, J.M. and Hickson, C.J. (1997): Physical and chemical volcanology of the Eocene Mount Clisbako volcano, central British Columbia (93B/12, 13; 93C/9, 16); in Interior Plateau Geoscience Project: Summary of Geological, Geochemical and Geophysical Studies, L.J. Diakow, P. Metcalfe and J. Newell, Editors, *BC Ministry of Energy, Mines and Petroleum Resources*, Paper 1997-2, pages 31–61.
- Mihalynuk, M.G., Erdmer, P., Ghent, E.D., Cordey, F., Archibald, D.A., Friedman, R.M. and Johannson, G.G. (2004): Coherent French Range blueschist: subduction to exhumation in <2.5 m.y.?; *Geological Society of America*, Bulletin, Volume 116, pages 910–922.
- Mihalynuk, M.G., Peat, C.R., Terhune, K. and Orovan, E.A. (2008a): Regional geology and resource potential of the Chezacut map area, central British Columbia (NTS 093C/08); in Geological Fieldwork 2007, *BC Ministry of Energy, Mines and Petroleum Resources*, Paper 2008-1, pages 117–134, URL <<http://www.empr.gov.bc.ca/DL/GSBPubs/GeoFldWk/2007/13-Mihalynuk-Chezacut34526.pdf>> [November 2008].
- Mihalynuk, M.G., Peat, C.R., Orovan, E.A., Terhune, K., Ferbey, T. and McKeown, M.A. (2008b): Chezacut area geology (NTS 93C/8); *BC Ministry of Energy, Mines and Petroleum Resources*, Open File 2008-2, scale 1:50 000, URL <<http://www.empr.gov.bc.ca/Mining/Geoscience/PublicationsCatalogue/OpenFiles/2008/Pages/2008-2.aspx>> [November 2008].
- Mihalynuk, M.G. and Friedman, R.M. (2009): First isotopic age constraints for the Dean River Metamorphic belt, Anahim Lake area: implications for crustal extension and resource evaluation in west-central British Columbia; in Geological Fieldwork 2008, *BC Ministry of Energy, Mines and Petroleum Resources*, Paper 2009-1, pages 101–108.
- MINFILE (2007): MINFILE BC mineral deposits database; *BC Ministry of Energy, Mines and Petroleum Resources*, URL <<http://www.minfile.ca>> [November 2007].
- Mustard, P.S. and MacEachern J.A. (2007): A detailed facies (sedimentological and ichnological) evaluation of archived hydrocarbon exploration drill core from the Nechako Basin, BC; in The Nechako Initiative-Geoscience Update, *BC Ministry of Energy, Mines and Petroleum Resources*, Petroleum Geology Open File 2007-1, pages 7-57, URL <http://www.empr.gov.bc.ca/OG/oilandgas/petroleumgeology/ConventionalOilAndGas/InteriorBasins/Documents/The_Nechako_Initiative-Geoscience_Update_2007.pdf> [November 2008].
- Mustard, P.S. and Van der Heyden, P. (1997): Geology of the Tatla Lake and east half of Bussel Lake; in Interior Plateau Geoscience Project: Summary of Geological, Geochemical and Geophysical Studies, L.J. Diakow, P. Metcalfe and J. Newell, Editors, *BC Ministry of Energy, Mines and Petroleum Resources*, Paper 1997-2, pages 103–122.
- Pálffy, J., Smith, P.L. and Mortensen, J.K. (2000): A U-Pb and ⁴⁰Ar-³⁹Ar time scale for the Jurassic; *Canadian Journal of Earth Sciences*, Volume 37, pages 923–944.
- Ricketts, B.D., Evenchick, C.A., Anderson, R.G. and Murphy, D.C. (1992): Bowser Basin, northern British Columbia; constraints on the timing of initial subsidence and Stikinia-North America terrane interactions; *Geological Society of America*, Geology, Volume 20, pages 1119–1122.
- Riddell, J.M. (2006): Geology of the southern Nechako Basin (NTS 92N, 92O, 93C, 93F, 93G), sheet 3 of 3-geology with contoured gravity underlay; *BC Ministry of Energy, Mines and Petroleum Resources*, Petroleum Geology Map 2006-1, scale 1:400 000.
- Riddell, R. and Ferri, F. (2008): Nechako Project Update; in Geoscience Reports 2008, *BC Ministry of Energy, Mines and Petroleum Resources*, pages 67–77.
- Riddell, J.M., Ferri, F., Sweet, A.R. and O'Sullivan, P.B. (2007): New geoscience data from the Nechako Basin project; in The Nechako Initiative-Geoscience Update 2007, *BC Ministry of Energy, Mines and Petroleum Resources*, Petroleum Geology Open File 2007-1, pages 59–98, URL <http://www.empr.gov.bc.ca/OG/oilandgas/petroleumgeology/ConventionalOilAndGas/InteriorBasins/Documents/The_Nechako_Initiative-Geoscience_Update_2007.pdf> [November 2008].
- Shives, R.B.K. and Carson, J.M. (1994): Multiparameter airborne geophysical survey of the Clisbako River area, Interior Plateau, British Columbia (parts of 093 B/12, 93 C/9, 93 C/16); *Geological Survey of Canada*, Open File 2815, 56 pages, URL <http://edg.rncan.gc.ca/geochem/metadata_rel_e.php?rel=of02815> [November 2008].
- Shore, T.L. and Safranyik, L. (1992): Susceptibility and risk rating systems for the mountain pine beetle in lodgepole pine stands; *Forestry Canada*, Pacific Forestry Centre, Information Report BC-X-336, 17 pages, URL <http://bookstore.cfs.nrcan.gc.ca/detail_e.php?catalog=3155>.
- Spratt J. and Craven J. (2008): A first look at the electrical resistivity structure in the Nechako Basin from magnetotelluric studies west of Nazko, B.C. (NTS 092 N, O; 093 B, C, F, G); in Geoscience Reports 2008, *BC Ministry of Energy, Mines and Petroleum Resources*, pages 119–127.
- Stacey, J.S. and Kramer, J.D. (1975): Approximation of terrestrial lead isotope evolution by a two-stage model; *Earth and Planetary Science Letters*, Volume 26, pages 207–221.
- Stewart S.A. and Argent J.D. (2000): Relationship between polarity of extensional fault arrays and presence of detachments; *Journal of Structural Geology*, Volume 22, Number 6, pages 693–711.
- Taylor, S.W. (1999): 100 years of federal forestry in British Columbia; *Forest History Association of British Columbia*, BC Forest History Newsletter, Number 57, pages 1–7.
- Taylor, S.W. and Carroll, A.L. (2004): Disturbance, forest age, and mountain pine beetle outbreak dynamics in BC: a historical perspective; in Mountain Pine Beetle Symposium: Challenges and Solutions, T.L. Shore, J.E. Brooks and J.E. Stone, Editors, Natural Resources Canada, Canadian Forest Service, *Pacific Forestry Centre*, Information Report BC-X-399, pages 41–51.
- Tipper, H.W. (1969a): Geology, Anahim Lake; *Geological Survey of Canada*, Map 1202A, scale 1:253 440.
- Tipper, H.W. (1969b): Mesozoic and Cenozoic geology of the northeast part of Mount Waddington map-area (92N), Coast District, British Columbia; *Geological Survey of Canada*, Paper 68-33, 103 pages.
- Tipper, H.W. (1971): Surficial geology, Anahim Lake; *Geological Survey of Canada*, Map 1289A, scale 1:250 000.
- Thorkelson, D.J. and Rouse, G.E. (1989): Revised stratigraphic nomenclature and age determinations for mid-Cretaceous volcanic rocks in southwestern British Columbia; *Canadian Journal of Earth Sciences*, Volume 26, pages 2016–2031.
- van der Heyden, P. (2004): Uranium-lead and potassium-argon ages from eastern Bella Coola and adjacent parts of Anahim Lake and Mount Waddington map areas, west-central British Columbia; in Current Research 2004, *Geological Survey of Canada*, Paper 2004-A2, 14 pages.

ERRATUM

LEGEND	
<i>Neogene</i>	
●	Anahim belt volcanic rocks
●	Chilcotin Group
<i>Eocene Ootsa Lake Group</i>	
▲	Mount Sheringham pyroxene dacite
▲	Vitreous black dacite
▲	Dacite ash-flow
▲	Acicular hornblende dacite
▲	Dacite ash-flow (with biotite)
<i>Intrusive rocks</i>	
◆	Tatla Lake Stock
◆	Chilanko Intrusive Complex

Legend for figure 7 omitted from the original published volume.